Covalent Interaction

Jan C. A. Boeyens

Abstract Reviewed in historical contect, bond order emerges as a vaguely defined concept without a clear theoretical basis. As an alternative, the spherical standing-wave model of the extranuclear electronic distribution on an atom provides a simple explanation of covalent bond order as arising from the constructive and destructive interference of wave patterns. A quantitative measure derives from a number pattern that relates integer and half-integer bond orders through series of Fibonacci numbers, consistent with golden-spiral optimization. Unlike any previous definition of bond order this approach is shown to predict covalent bond length, dissociation energy and stretching force constants for homonuclear interactions that are quantitatively correct. The analysis is supported by elementary number theory and involves atomic number and the golden ratio as the only parameters. Validity of the algorithm is demonstrated for heteronuclear interactions of any order. An exhaustive comparison of calculated dissociation energies and interatomic distance in homonuclear diatomic interaction, with experimental data from critical review, is tabulated. A more limited survey of heteronuclear interactions confirms that the numerical algorithms are generally valid. The large group of heteronuclear hydrides is of particular importance to demonstrate the utility of the method and molecular hydrogen is treated as a special case. A simple formula that describes the mutual polarization of heteronuclear pairs of atoms, in terms of valence densities derived from a spherical-wave structure of extranuclear electronic charge, is used to calculate the dipole moments of diatomic molecules. Valence density depends on the volume of the valence sphere as determined by the atomic ionization radius, and the interatomic distance is determined by the bond order of the diatomic interaction. The results are in satisfactory agreement with literature data and should provide a basis for the calculation of more complex molecular dipole moments. The diatomic CO is treated as a special case, characteristic of all interactions traditionally identified as dative bonds.

Jan C. A. Boeyens
Unit for Advanced Scholarship, University of Pretoria, South Africa.
e-mail: jan.boeyens@up.ac.za

Keywords: bond order, dipole moment, force constant, general covalence, ionization radius, golden ratio

1 Introduction

The simplest model of a covalent bond is based on an electrostatic point-charge simulation of overlapping spherical valence-electron charge clouds that surround monopositive atomic cores. For a homonuclear pair of atoms with radius r and internuclear distance d the dissociation energy, D is calculated from

$$D' = \varepsilon^2 \left(\frac{3}{d'} - \frac{1}{2-d'} \right) \tag{1}$$

where

$$\varepsilon = \frac{3V_0}{4\pi r^3} = 1 - \frac{3d'}{4} + \frac{(d')^3}{16}, \tag{2}$$
$$d' = d/r,$$

the common volume between the overlapping spheres,

$$V_0 = \pi \left[\frac{4}{3} r^3 - r^2 d + \frac{d^3}{12} \right]$$

and $D = KD'/r$.

On equating the atomic radius to a characteristic atomic radius, r_a, a single curve of d' *vs* D' describes homonuclear covalent interaction, irrespective of bond order. Practical use of the formulae requires definition of a complex set of characteristic radii, which could be derived empirically [1] and was used subsequently to calculate molecular shape descriptors [2] and as the basis of a generalized Heitler-London procedure, valid for all pairwise covalent interactions [3, 4]. In all of these applications interaction is correctly described by the dimensionless curves of Fig. 1.

For heteronuclear interaction using dimensionless distances $d' = d/R$, $R = \sqrt{r_1 r_2}$ and $r_1/r_2 = x$, the overlap formulae are:

$$D' = \delta\varepsilon \left\{ \frac{1}{d'} \left[\frac{x^2 - 2x + 4}{(2-x)x} \right] - \frac{1}{(1+x)/\sqrt{x} - d'} \right\} \tag{3}$$
$$\delta\varepsilon = \left[T_3 - \frac{3T_2}{16d'} - \frac{3}{4} T_1 d' + \frac{1}{16}(d')^3 \right]^2$$

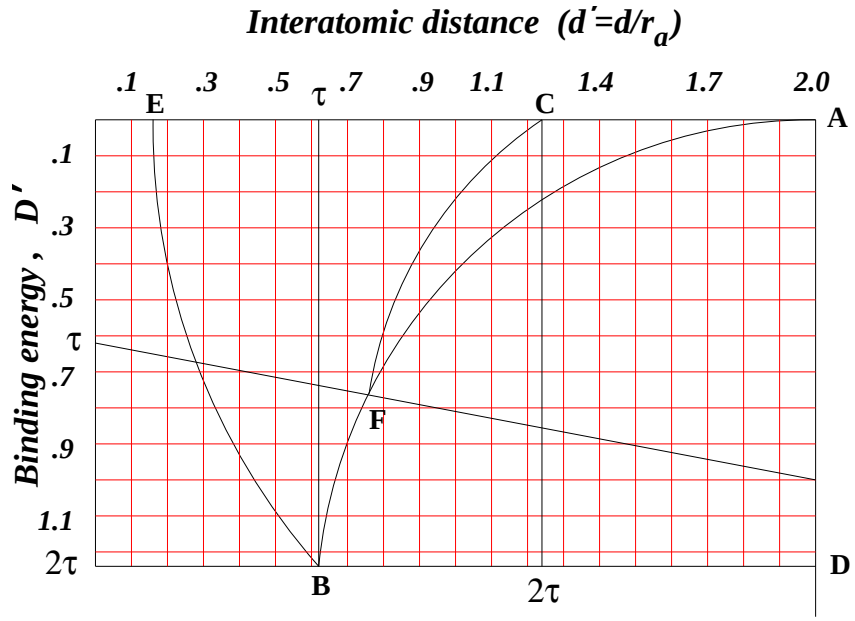

Fig. 1 Covalence curves in dimensionless units. Homonuclear interactions are described by the curve BFC and heteronuclear interactions map into the crescent CFA.

$$T_1 = \frac{1}{2}\left[x + \frac{1}{x}\right]$$
$$T_2 = x^2 + \frac{1}{x^2} - 2$$
$$T_3 = \frac{1}{2}\left[x^{3/2} + x^{-3/2}\right]$$

The general covalence curve, first calculated by the point-charge electrostatic model, has a simple geometrical construction [5] within a golden rectangle of size $2 \times 2\tau$. The limiting covalence curve AB is a semi-circle centred on the extension of AD at the point (2,9τ/4=1.39). It is intersected at F by the homonuclear semi-circle through point C and centred at coordinates (2,1). Homonuclear interactions map to this curve up to the point where it intersects AB, then follow this curve to B. All points (d', D') that characterize heteronuclear covalent bonds lie within the crescent between the two curves. The circular segment BE is centred at A.

The relationship between interatomic distance and dissociation energy of atoms in interaction has an interesting connection with the golden ratio, but is of limited use without an empirical set of characteristic atomic radii. All efforts to derive such radii from atomic properties have been unsuccessful for the simple reason that these radii are not free-atom properties. However, the search has resulted in the identification of an useful set of free-atom radii, characteristic of the atomic valence state [6].

Whereas the interaction radii, r_a describe the relationship between interatomic distance and dissociation energy, free-atom valence radii predict these quantities separately, but related *via* bond order, which is defined precisely in terms of interfering spherical electron waves. In this paper we show how these predictions agree quantitatively with available spectroscopic, crystallographic and thermodynamic data. All observed bond lengths, dissociation energies and stretching force constants are taken from the tables in HCP [7].

2 The Bond-order Concept

The bond-order concept developed from the notion of multiple bonding, which was formulated empirically towards the end of the 19th century, to explain the composition of organic compounds. The basic rule of thumb, proposed by August Kekulé [8], was to assign valences of 1 through 4 to H, O, N and C respectively. In order to rationalize the observed composition of ethylene, acetylene and benzene it was necessary to postulate the formation of double, triple and $1\frac{1}{2}$-order carbon-carbon bonds in these compounds.

This scheme could be extended in a natural way to O, N, S, P, Cl, *etc*. To bring the scheme into line with the stereochemical ideas of Le Bel and van't Hoff, valences came to be associated with *affinity centres*, arranged tetrahedrally in the surface of spherical atoms. The formation of single to triple bonds was explained on this basis by Victor Meyer [9, 10] as the touching of atomic spheres in different mode, as shown in Fig. 2.

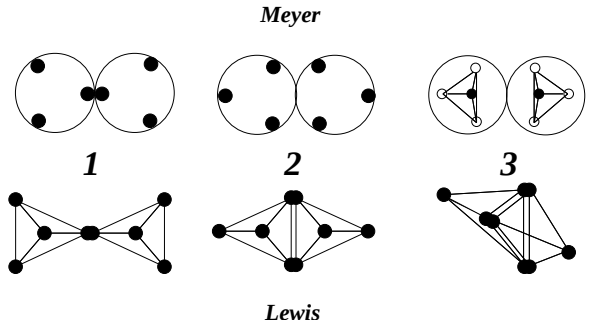

Fig. 2 Bond orders distinguished in terms of affinity centres (top) and electron pairs (bottom)

Whereas the atomic centres remain at the same distance from each other, the affinity centres move progressively further apart as the bond order increases, predicting weaker interaction.

Based on Sommerfeld's atomic model [11] of elliptic orbits, directed towards the corners of a cube, a number of chemists, including Kossel, Lewis, Langmuir and

Bury, developed an electronic theory to account for atomic structure and valency at the same time. To account for the periodic table of the elements, Rydberg's formula for the atomic number of an inert gas

$$N = 2(1^2 + 2^2 + 2^2 + 3^2 + 3^2 + 4^2 \ldots)$$

had to be reconciled with spectroscopic evidence, supported by Sommerfeld's atomic model, which predicted the number of electrons per shell as equal to the square of the principal quantum number, *i.e.* n^2, $n = 1, 2, 3 \ldots$. Instead of assuming that by increasing the number of electrons, atomic shells would become occupied to saturation in the order of increasing n, it was postulated that the completion of the next octet (at the corners of a cube) takes priority over saturation of the shell.

In the case of covalent interaction the octet is of primary importance, next to the role of electron pairs, implied by the factor 2 in Rydberg's formula, from which two-fold symmetry in the electronic configuration of an atom was inferred. It is important to note that the classification of electrons into *s*, *p*, *d*, *f* subsets, characterized by four quantum numbers in terms of Pauli's exclusion principle, which states that no two electrons in one atom can have all four quantum numbers identical, antedates the development of wave mechanics.

In line with van't Hoff's stereochemistry and the orientation of elliptic orbits, covalent bonds could be represented by tetrahedra that touch in apical, edgewise and facial mode, involving one, two or three electron pairs in an interaction, also shown in Fig. 2. This theory predicts increased bond strength with increasing bond order, but fails to account quantitatively for observed internuclear distances. For example, this model predicts the interatomic distances in methane and acetylene in the ratio of 3:1.

Occurrence of the stereo isomers, known as maleic and fumaric acids, has been interpreted for a long time as evidence of a barrier to rotation around a double bond. It is of interest to note that this steric rigidity is consistent with the orientation of Victor Meyer's affinity centres and with the Lewis model of electron pairs.

The definition of bond order as the number of electron pairs shared between two atoms is still widely accepted today, but the geometry of interaction has been adapted to the theory of orbital hybridization, to be considered next.

2.1 Orbital Hybridization

Schrödinger's rationalization of atomic spectra and integral quantum numbers, in terms of a wave model, introduced an improved mathematical description of the electronic configuration of atoms, derived empirically before. Unfortunately the theory was not developed to its full potential because of reluctance to abandon the classical concept of sub-atomic particles.

The coming of wave mechanics, which should have been hailed as final vindication of the proposed wave nature of electrons, already surmised and soon to be

demonstrated experimentally at the time, was successfully resisted as inadequate to account for cloud-chamber trajectories and the Compton effect. Although both objections are spurious they had such authority in support that an illogical watered-down re-interpretation of Schrödinger's model gained universal acceptance. The consequences for theoretical chemistry have been disastrous.

In summary, Schrödinger managed to solve a differential equation that describes the motion of an electron in the central field of a proton, as in the hydrogen atom, in wave formalism. By separating the radial and angular components of the wave function three quantum numbers, essentially equivalent to those of Sommerfeld, were obtained without further assumption. The three quantum numbers, which obey the exclusion principle, are conveniently summarized as:

$$\begin{aligned} n &= 1,2,3,\ldots \\ l &= 0,1,\ldots,(n-1) \\ m_l &= -l,\ldots,+l \end{aligned}$$

in conjunction with the empirically added spin quantum number, $m_s = \pm\frac{1}{2}$. In physical interpretation the principal quantum number, n, specifies the eigenvalues of the electronic energy, whereas l and m_l specify the eigenvalues of orbital angular momentum and its value in a magnetic field, respectively.

Although the Schrödinger solution is demonstrably superior to the Sommerfeld model it lacks the pictorial appeal of the Lewis tetrahedral model. Still, there was the general belief, articulated by Linus Pauling [12] that,

> ... if quantum theory had been developed by the chemist rather than the spectroscopist it is probable that the tetrahedral orbitals described below would play the fundamental role in the theory, in place of the *s* and *p* orbitals.

The chemist has not succeeded in doing this. Pauling himself proposed the scheme of orbital hybridization as a quantum theory of covalent interaction. Despite its uncritical acceptance for many years this approach is shown by elementary reasoning to be in direct conflict with the fundamentals of quantum theory.

It starts with a degenerate set of orbital angular momentum vectors with quantum numbers $l = 1$, $m_l = -1,0,1$, which in cartesian coordinates may be formulated as

$$p^{-1} = \frac{x-iy}{r} \quad ; \quad p^0 = \frac{z}{r} \quad ; \quad p^1 = \frac{x+iy}{r}.$$

The use of complex quantities is avoided by making the linear combinations:

$$\tfrac{1}{2}(p^{-1}+p^1) = \frac{x}{r} \quad ; \quad \tfrac{1}{2}(p^1-p^{-1}) = \frac{iy}{r}.$$

The overall result is clearly equivalent to the new set:

$$p^{-1} = \frac{z-iy}{r} \quad ; \quad p^0 = \frac{x}{r} \quad ; \quad p^1 = \frac{z+iy}{r},$$

which represents a simple rotation of the coordinate axes.

Pauling however, preferred a different interpretation by defining

$$p_y = \frac{1}{2i}\left(p^1 - p^{-1}\right) = \frac{y}{r},$$

in order to generate a degenerate set of real $p-''$orbitals$''$,

$$p_x = \frac{x}{r} \quad ; \quad p_y = \frac{y}{r} \quad ; \quad p_z = \frac{z}{r},$$

directed along the cartesian axes. This procedure destroys the complex entanglement of the non-classical variables, demanded by quantum theory, to produce three orthogonal functions with $m_l = 0$, in violation of the exclusion principle, which is not required in classical systems. Efforts to associate electron spin with real obitals are therefore meaningless.

No amount of handwaving can circumvent this conclusion. The elaborate procedure whereby these orbitals are incorporated in further $''$hybridization$''$ to define the combinations sp^3, sp^2 and sp to simulate tetrahedral, trigonal and linear sets of orbitals, is likewise without quantum-mechanical meaning [13]. At best, it amounts to a classical reconstruction of these geometries. In short, the well-known procedure to define bond order and steric rigidity in terms of overlapping σ and π orbitals is meaningless, representing no more than the Lewis model, in more dignified jargon. The fanciful notion of π-overlap cannot explain why a triple bond should have no barrier to rotation, rather than twice the rigidity of a double bond.

2.2 Bond Order in Molecular Mechanics

The only successful simulation of molecular conformation, based on classical concepts, has become known as molecular mechanics. It relies on the ideas of chemical bonds free of strain and computerized minimization of the strain energy generated by distortion of the strain-free interactions in a molecule. In this application it is necessary to stipulate strain-free bond lengths for bonds of different order. Although such parameters can in many cases be derived empirically, a more fundamental theoretical prediction would, for obvious reasons, be preferred. Efforts to derive suitable parameters by the methods of quantum chemistry have been futile.

Important progress became possible on noting a simple relationship between interatomic distances in bonds of different order. The rationale behind the observation comes from the simple model of a covalent bond, seen as the situation of equilibrium between the electrostatic attraction of a pair of valence electrons to the nuclei and the internuclear repulsion. In the formation of higher-order bonds the role of those valence electrons in excess of bonding pairs may be seen as screening the internuclear repulsion [15]. The logic behind this interpretation is supported by the observation that, given the details of any bond, addition of a universal screening constant to the interaction, transforms the single bond into a bond of specified higher order, irrespective of the atoms involved.

In practice calculations have been performed in two different ways. Given the bond length, dissociation energy and stretching force constant characteristic of the single bond, the interaction is described by a Morse function. If this function is modified by addition of a term that represents screening of the internuclear repulsion, the relevant Morse curve of the higher-order bond is obtained [16]. Alternatively, the potential-energy curve, calculated by the Heitler-London method [3], is modified in the same way, using the same screening factors, to simulate higher bond orders.

Heitler-London simulation of general covalence depends on a set of characteristic atomic radii, assumed to describe a single electron in the valence state. Such radii were obtained empirically, in the first instance, by point-charge simulation of covalent interaction [17]. A more satisfactory derivation of atomic radii was discovered in the simulated compression of atoms in Hartree-Fock calculations, resulting in ionization at a characteristic compression, closely related to the empirical radii [18].

These ionization radii, which have been shown [19] to underpin the electronegativity concept, have recently been derived by an extremely simple and more reliable simulation of atomic structure as a standing electronic wave packet [6]. This simulation, which is free of the errors of approximation that affect the HF simulation of small atoms, has produced a more reliable set of ionization radii, suitable for direct prediction of interatomic distance in general pairwise interaction within bonds of any order. The procedure is outlined in the next section.

2.3 Bond Order from Ionization Radii

Comparison of the interatomic distances (d) reported for homonuclear covalent interactions, commonly considered to be first order, revealed a remarkable relationship with the corresponding ionization radii, r_0. Using data from HCP [7], the large majority of bond lengths, defined in dimensionless units as $d' = d/r_0$ had $d' = 0.868$, with little variation. A few notable exceptions occurred for F–F, O–O and I–I, with $d' = 0.932$. Supporting evidence for typical interactions is shown in Table 1.

On repeating the exercise for traditional second-order bonds a similar result of $d' = 0.764$ is obtained. For third-order bonds, with an admittedly smaller sample one calculates $d' = 0.680$. Using the observed bond length of benzene one finds $d' \simeq 0.786$ for the bond of assumed $1\frac{1}{2}$ order. Extending the search to homonuclear transition-metal diatomic molecules where high-order bonds are common, and to diatomic alkali metals with assumed bond orders of zero, a complete set of dimensionless bond lengths, in good agreement with experiment was established for all orders.

If we define zero bond order to occur at $d = r_0$, *i.e.* $d' = 1$, an interesting variation with bond order, from unity to the golden ratio, $\tau = 0.61803...$ is inferred. This variation is reminiscent of the convergence of the ratio $Z/(A-Z)$, of protons to neutrons in stable nuclides, that leads to the generalized periodic function of atomic matter [20]. Using this as a cue the variation of bond length with bond order can

Table 1 Calculated interatomic distance for low-order homonuclear interactions

	C	N	O	F
r_0/Å	1.78	1.69	1.60	1.52
$d(X-X)$	1.545	1.467	1.491	1.417
Expt.	1.54	1.47	1.48	1.41
	Si	P	S	Cl
r_0/Å	2.62	2.51	2.47	2.30
$d(X-X)$	2.274	2.179	2.144	1.996
Expt.	2.32	2.21	2.05	1.99
	Ge	As	Se	Br
r_0/Å	2.89	2.80	2.71	2.61
$d(X-X)$	2.51	2.43	2.35	2.27
Expt.	2.41	2.44	2.32	2.28
	Sn	Sb	Te	I
r_0/Å	3.19	3.09	2.98	2.88
$d(X-X)$	2.77	2.68	2.59	2.68
Expt.			2.59	2.67

be specified as a power series in τ. In fact, any power $n > 6$, with integers j_b as coefficients defines bond order b, by $d' = j_b\tau^n$, as shown in Table 2.

Table 2 Any power of the golden ratio, τ^n with covariant j_b, tabulated in bold script, as coefficients, predicts the ratio $d/r_0 = d' = j_b\tau^n$, which determines the dimensionless bond length of order b. The different coefficients for consecutive bond orders are related by the Fibonacci numbers Δj

Order,b	τ^4	τ^5	τ^6	τ^7	τ^8	τ^9	τ^{10}	τ^{11}	τ^{12}	τ^{13}
4	**4**	**7**	**11**	**18**	**29**	**47**	**76**	**123**	**199**	**322**
Δj			1	1	2	3	5	8	13	21
$3\frac{1}{2}$			**12**	**19**	**31**	**50**	**81**	**131**	**212**	**343**
Δj				1	1	2	3	5	8	13
3				**20**	**32**	**52**	**84**	**136**	**220**	**356**
Δj			1	1	2	3	5	8	13	21
$2\frac{1}{2}$	**5**	**8**	**13**	**21**	**34**	**55**	**89**	**144**	**233**	**377**
Δj			1	1	2	3	5	8	13	21
2			**14**	**22**	**36**	**58**	**94**	**152**	**246**	**398**
Δj			1	1	2	3	5	8	13	21
$1\frac{1}{2}$			**15**	**23**	**38**	**61**	**99**	**160**	**259**	**419**
Δj		1	1	2	3	5	8	13	21	34
1		**9**	**16**	**25**	**41**	**66**	**107**	**173**	**280**	**453**
Δj		1	1	2	3	5	8	13	21	34
$\frac{1}{2}$		**10**	**17**	**27**	**44**	**71**	**115**	**186**	**301**	**487**
Δj		1	1	2	3	5	8	13	21	34
0	**7**	**11**	**18**	**29**	**47**	**76**	**123**	**199**	**322**	**521**

The coefficients for given bond order increase like a Fibonacci series with increasing n. This is immediately obvious for the coefficients of bond orders 4 and 0, which correspond, in both cases, to the familiar Lucas numbers. This correspondence is interpreted to define a closed, and hence periodic, system, consistent with the assumed spherical wave structure of a valence electron. By noting how Δj_b for any pair of consecutive bond orders also defines a Fibonacci series with increasing n, the appropriate coefficients for any power can be specified directly without calculation. The empirically derived bond-order scale factors d' are then seen to be integral multiples of τ^n. It could be of special significance in the analysis of aromatic interactions to note that $d'(0) = \tau^0$, $d'(1\frac{1}{2}) = 1/(2\tau)$ and $d'(4) = \tau$. The sufficiently converged values of $j_b\tau^{13}$ are shown in Table 3.

Table 3 Definition of d', derived from r_0 for different bond orders. The relative overlap volume ε appears quantized in units of $n/40$. The columns on the right are discussed in the next section

Order	d'	ε	$n/40$	$n(2)$	$n(3)$	$n(4)$	$n(5)$	$n(6)$
0	1.000	0.3	12	7	10	10	11	11
$\frac{1}{2}$	0.935	0.35	14	6	8	9	10	10.5
1	0.869	0.4	16	5	7	8	9.5	10
$1\frac{1}{2}$	0.804	0.425	17	4.5	6.5	7.5	9	9.5
2	0.764	0.45	18	4	6	7	8.5	9
$2\frac{1}{2}$	0.724	0.475	19					8.5
3	0.683	0.50	20	3			8	8
$3\frac{1}{2}$	0.658	0.525	21				7.5	7.5
4	0.618	0.55	22				7	7

With reference to the point-charge simulation of covalent interaction we note that the common volume between two overlapping spheres of radius r, with centres at a distance d apart, is calculated as

$$V_0 = \pi\left[\frac{4}{3}r^3 - r^2 d + \frac{d^3}{12}\right],$$

or, in dimensionless units of $d' = d/r$, the relative overlap volume,

$$\varepsilon = \frac{3V_0}{4\pi r^3} = 1 - \frac{3d'}{4} + \frac{(d')^3}{16}. \qquad (2)$$

This quantity, also listed in Table 3, is seen to assume quantized values of $n/40$ for the common bond orders.

2.4 Dissociation Energy and Bond Order

It is generally accepted that there is some inverse relationship between covalent bond length (d) and dissociation energy (D). The point-charge model of covalent interaction defines this relationship in terms of a smooth curve (Fig. 1) which represents all homonuclear diatomic interactions on expressing distance and energy in special dimensionless units, defined by $d' = d/r_0$, $D' = Dr_0/K$, where K is a dimensional constant. For D in kJmol^{-1} or eV respectively $K = 1389$ or 14.35. Having shown that the bond order-related linearity $d = j_b r_0 \tau^n$ is generally obeyed, we infer fixed values of d' for all bonds of order b.

The observed relationship between the common volume, defined by overlapping charge spheres, and bond order, shown in Table 3, suggests a direct relationship between bond order and dissociation energy. Noting the connection with spherical volume we look for a dependence of the type

$$\frac{D_x r_0}{K} = D' \propto r_0^3$$

and find that first-order homonuclear interactions for *p*-block elements obey the rule

$$D' = r_0^3 \tau^n \quad , \quad i.e. \quad D_x = K r_0^2 \tau^n. \tag{4}$$

The values of n, which produce dissociation energies, D_c, to match experimental data D_x, correlate positively with bond orders derived from interatomic distances. Some results are shown in Table 4. Results for some higher order bonds, in the format $\mathrm{A}(n) : D_c(D_x)$ include:
C(4):642(600); C(3.16):964(966); N(3):937(945); O(4):519(498)
S(6):472(425); As(7):374(382); Se(7):351(331); C(4.5):505(479 in biphenyl)

Within a periodic family, interactions with common n have equal bond orders. Calculated n, for first-order interaction, increases stepwise from $n = 5, 6$ for second period elements, to $n = 10$ for period 6. We find $n = 5$ for C and $n = 6$ for N, O, F, previously identified to form $\frac{1}{2}$ order bonds. For second and third-order interactions, within a given period, the appropriate exponents are $n_2 = n_1 - 1$ and $n_3 = n_1 - 2$. This rule would restrict golden exponents to integers and half integers. All interactions with $d > r_0$ are traditionally described as non-bonded.

Bond-by-bond data to compare calculated parameters with experiment are presented in sections 3 and 4.

2.5 Stretching Force Constants

The relationship between bond order and dimensionless interatomic distance is represented by three linear functions over the intervals $b = (0, 1\frac{1}{2})$, $(1\frac{1}{2}, 3)$ and (3,4) as shown in Fig. 2.

Table 4 Dissociation energies ($kJmol^{-1}$) and exponents n for lowest-order homonuclear observed interactions in the s and p blocks.

	Li	Be			B	C	N	O	F
r_0/Å	2.36	2.20			1.88	1.78	1.69	1.60	1.52
n	9	10			6	5	6	6	6
D_c	102	54			273	397	221	198	179
D_x	110	59			290	377	252	214	159
	Na	Mg			Al	Si	P	S	Cl
r_0	3.09	2.87			2.74	2.62	2.51	2.47	2.30
n	11	12			9	7	6	7	7
D_c	66	35			138	328	487	292	253
D_x	75	11			133	310	485	286	243
	K	Ca	Cu	Zn	Ga	Ge	As	Se	Br
r_0	3.50	3.08	2.88	3.11	3.00	2.89	2.80	2.71	2.61
n	12	13	8.5	13	10	8	8	8	8
D_c	53	25	192	22(6)	100	247	232	217	202
D_x	57	~ 17	201	22	< 106	264	181	223	194
	Rb	Sr	Ag	Cd	In	Sn	Sb	Te	I
r_0	3.81	3.54	3.11	3.00	3.31	3.19	3.09	2.98	2.88
n	13	14	9	15	11	9	8	8	9
D_c	38	21	163	7	76	186	282	263	152
D_x	49	16	159	7	82	187	302	258	153
	Cs	Ba	Au	Hg	Tl	Pb	Bi		
r_0	4.03	3.75	3.38	3.24	3.43	3.32	3.22		
n	13		9	15	12	11	9		
D_c	43		209	10	51	77	190		
D_x	44		226	8	63	87	197		

The different slopes correspond to the differential change of d with respect to b and hence describe the response of bond order to increasing d, commonly defined as a stretching force constant:

$$\tfrac{1}{2}k_r = \frac{\Delta D'}{(\Delta d')^2},$$

In molecular mechanics the usual practice is to specify energies in units of $kJmol^{-1}$, interatomic distance in Å and k_r in Ncm^{-1} (≡mdyne/Å). In these units

$$k_r = \frac{2\Delta D' \times K \times 10^{-2}}{6.2 r_0 (r_0 d')^2} = \frac{K\Delta D'}{301(\Delta d')^2 r_0^3}$$
$$= \frac{4.615\Delta D'}{(\Delta d')^2 r_0^3} \quad \mathrm{Ncm}^{-1} \tag{5}$$

For interactions of known bond order the quantities $\Delta d'$ for a stretch to lower order follow directly from Table 1, provided it occurs in a region of uniform slope. Energy differences are in general proportional to $\Delta D = \tau^n - \tau^{n+1} = \tau^{n+2} = \tau^+$. As bond order is not an absolute measure, only relative slopes can be stipulated. Also,

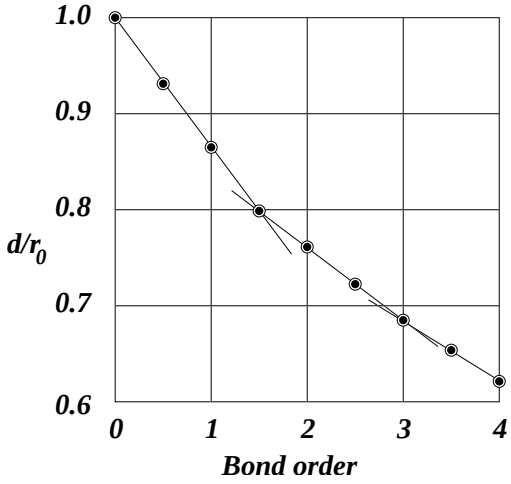

Fig. 3 Variation of interatomic distance (d') with bond order

whereas d' may change continuously, bond order changes in discrete steps, determined by the interference of standing waves. We therefore assume that equation (5) correctly describes a hypothetical linear response for a stretch from bond order four ($d' = 0.6$) to zero, with a slope of 0.1 measured in Fig.3. For any intermediate stretch of different slope σ, a multiplicative scale factor, that represents an effective slope of $s = \sigma/0.1$ is added to eqaution (5).

The procedure is illustrated by calculating the stretching force constant of diatomic C_2, considered of bond order $2\frac{1}{2}$, such that:

$$k_r = \frac{4.615 \times (\tau^{5.5} = 0.0709)}{(0.080 \times 1.78)^2} \times 0.8 = 12.59 \quad \text{Ncm}^{-1}$$

The scale factor of 0.8 represents the slope. Note that the stretch is considered to operate between bond orders $2\frac{1}{2}$ and $1\frac{1}{2}$, *i.e.* $n = 3.5 \leftarrow 4.5$, $\Delta D \propto \tau^{5.5}$. This result is in good agreement with the experimental 12.16 Ncm^{-1}.

As a further test the force constant of third order N_2 $(\tau^+ = \tau^{3+2})$ follows as

$$k_r = \frac{4.615 \times 0.0902}{(0.081 \times 1.69)^2} = 22.2 \quad \text{Ncm}^{-1},$$

in exact agreement with experiment.

Calculation of k_r for $\text{C}\overset{2}{=}\text{C}$ is complicated by the change of slope between orders 2 and 1. This is readily compensated for by graphical recalculation of $\Delta d' = 0.093$ and mean slope of 0.93:

$$k_r = \frac{4.615 \times 0.0554}{(0.093 \times 1.78)^2} \times 0.93 = 8.68 \quad \text{Ncm}^{-1}$$

in good agreement with the value of 8.43 $\mathrm{Ncm^{-1}}$ measured for $CCl_2{=}CH_2$.

For $C\overset{1}{—}C$ the energy difference is obtained from $\tau^5 - \tau^{6.5} = 0.0464$ and

$$k_r = \frac{4.615 \times 0.0464}{(0.131 \times 1.78)^2} \times 1.3 = 5.12 \quad \mathrm{Ncm^{-1}}.$$

The force constant calculated from the vibrational frequency ω_e of ethane is $k_r = 4.50$ $\mathrm{Ncm^{-1}}$.

For F_2 the energy difference $\tau^5 - \tau^6 = \tau^7$ occurs against a calculated force constant $k_r = 5.2$, compared to the experimental 4.7 $\mathrm{Ncm^{-1}}$.

The calculated force constant for O_2 is obtained from $\Delta d' = 0.093$, $n^+ = 6$ as $k_r = 10.79$, compared to the observed 11.77 $\mathrm{Ncm^{-1}}$.

Extension of the calculation to higher periods relies on the wave model of atomic electron density. Changes in bond order are interpreted as stepwise changes in the pattern of overlap between the electronic wave structures of interacting atoms. The effect on interatomic distance depends on the wavelength of the interfering waves, which in turn depends on atomic volume as elaborated in section 2.6. In the second shell of 8 electrons $\Delta d' = 0.1306$ corresponds to unit change in bond order. At the next level with an additional 8 electrons a stretch of $\Delta d' = 0.0653$ suffices for relaxation to lower order[1]. With some empirical guidance we arrive at the unimodular sequence of factors 1, $\frac{1}{2}$, $\frac{2}{5}$, $\frac{1}{3}$, $\frac{1}{4}$ to effect a change of bond order at successive electronic levels. The scheme is demonstrated by the calculated force constants for diatomic halogens:

$$Cl_2 : \Delta d' = 0.0653, n^+ = 9, k_r = 2.7 \times 1.3 = 3.51 \quad (3.23\ \mathrm{Ncm^{-1}})$$
$$Br_2 : \Delta d' = 0.0522, n^+ = 10, k_r = 2.62 \quad (2.46\ \mathrm{Ncm^{-1}})$$
$$I_2 : \Delta d' = 0.0435, n^+ = 11, k_r = 1.91 \quad (1.72\ \mathrm{Ncm^{-1}})$$

Also on the second period:

$$Si_2 : \Delta d' = 0.0653, n^+ = 9, k_r = 2.71 \quad (2.15\ \mathrm{Ncm^{-1}})$$

and the second-order molecules

$$P_2 : \Delta d' = 0.093/2 = 0.0465, n^+ = 8, k_r = 5.78 \quad (5.56\ \mathrm{Ncm^{-1}})$$
$$S_2 : \Delta d' = 0.0465, n^+ = 8, k_r = 5.96 \quad (\mathrm{HCP} : 4.96\ \mathrm{Ncm^{-1}})$$

The reported value [7] for S_2 is obviously in error.

Quadruple dimetal interactions provide an interesting test:

[1] A bond is stretched by external forces, such as steric interactions, only until it flips spontaneously into the wave pattern that stabilizes lower bond order

$$\mathrm{Cr}_2 : \Delta d' = 0.0522, n^+ = 9, k_r = 2.45$$
$$\mathrm{Mo}_2 : \Delta d' = 0.0375, n^+ = 9, k_r = 4.08$$
$$\mathrm{Re}_2 : \Delta d' = 0.0375, n^+ = 9, k_r = 3.75$$
$$\mathrm{W}_2 : \Delta d' = 0.0375, n^+ = 9, k_r = 3.66$$

The effective slope in the high order region is close to unity. These results, in Ncm^{-1}, are in exact agreement with empirical molecular-mechanics simulations of these force constants [21, 22, 23].

2.6 Wave Model of Bond Order

The idea of covalent bond order is of special importance in the present instance, but not in its traditional form as the number of electron pairs shared between two atoms.

The familiar electron-pair exposition of bond order is that C, in the valence state, has 4 unpaired electrons after promotion of an *s* electron. In the case of N there is no room in the *p*-subshell to allow such promotion. However, the positive ion N^+, like C has four unpaired electrons and may form four single bonds as in NH_4^+. Oxygen has two unpaired electrons and is restricted to form either two single bonds or one double bond. The scheme works, but fails to account for the paramagnetism of dioxygen with known second-order bond strength. The experimental facts are consistent with neither of the following:

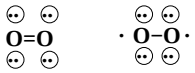

It is generally believed that the bonding in O_2 is correctly described in terms of molecular orbitals. However, this method, as traditionally formulated, argues the involvement of p_x, p_y and p_z orbitals, which have no physical meaning, and the bond order of dioxygen remains a mystery. This is the most glaring, but by no means the only, failure of the electron-pair definition of bond order.

The very idea of electron pairs, that presupposes point particles of charge, does not feature in the model of covalence proposed here. A plurality of electrons at the same energy level is considered instead as a single multiply-charged standing wave with quantized orbital angular momentum and spin. We propose that bond order of diatomic domains within molecules is quantized in a similar way and we look for a numerical sequence to account for the empirical regularity of Table 3. Prominence of the golden ratio in this formulation suggests a sequence based on Fibonacci fractions and/or the golden logarithmic spiral. This would render it self-similar to structures in the solar system, the periodic table of the elements and the electronic configuration of atoms.

As a first trial we consider a series of Fibonacci fractions in the range 1/1 to 3/5, to simulate bond orders between 0 and 4 ($d' = 1, \tau$). The unimodular sequence that converges to 1, *i.e.*:

$\frac{1}{1}$	$\frac{7}{8}$	$\frac{6}{7}$	$\frac{5}{6}$	$\frac{4}{5}$	$\frac{3}{4}$	$\frac{2}{3}$	$\frac{3}{5}$
1	0.875	0.857	0.833	0.8	0.75	0.667	0.6
0	1			$1\frac{1}{2}$	2	3	4

is immediately seen to reflect many features of the bond-order function.

An even better simulation, based on this sequence, is obtained by selecting suitable terms from a single Farey sequence, which means that all terms have the same denominator. This way we derive from $\mathscr{F}_{15}$ the sequence:

$\frac{1}{1}$	$\frac{14}{15}$	$\frac{13}{15}$	$\frac{4}{5}$	$\frac{11}{15}$	$\frac{2}{3}$	$\frac{3}{5}$	$\left(\frac{n}{15}, n = 9-15\right)$
1	0.933	0.867	0.8	0.733	0.67	0.60	
0	$\frac{1}{2}$	1	$1\frac{1}{2}$	2	3	4	

Starting from the next Fibonacci fraction, 5/8, $(\mathscr{F}_{16})$:

$\frac{1}{1}$	$\frac{15}{16}$	$\frac{7}{8}$	$\frac{13}{16}$	$\frac{3}{4}$	$\frac{11}{16}$	$\frac{5}{8}$	$\left(\frac{n}{16}, n = 10-16\right)$
1	0.938	0.875	0.81	0.75	0.688	0.625	
0	$\frac{1}{2}$	1	$1\frac{1}{2}$	2	3	4	

The next Fibonacci fraction predicts $(\mathscr{F}_{13})$:

$\frac{1}{1}$	$\frac{12}{13}$	$\frac{11}{13}$	$\frac{10}{13}$	$\frac{9}{13}$	$\frac{8}{13}$	$\left(\frac{n}{13}, n = 8-13\right)$
1	0.923	0.846	0.769	0.69	0.615	
0	$\frac{1}{2}$	1	2	3	4	

Starting from still higher Fibonacci fractions the same pattern persists, but gaps appear in the sequence of quantum numbers. The infinite sequence between 1 and τ is inferred to have the exact bond-order sequence, with large quantum numbers, embedded within it.

The most convincing simulation of bond order is from a golden logarithmic spiral with convergence angle of $\pi/8$, for integer orders, or $\pi/16$ to include half-integer orders, shown in Fig. 4. Bond orders 0 and 4 are separated by a right angle.

This simulation confirms the results of Table 3 in detail. As a matter of interest all of these bond orders are approximated in $\mathscr{F}_{34}$, which relates to the Fibonacci fraction 21/34, with a few gaps:

$\frac{1}{1}$	$\frac{15}{17}$	$\frac{29}{34}$	$\frac{27}{34}$	$\frac{13}{17}$	$\frac{25}{34}$	$\frac{23}{34}$	$\frac{11}{17}$	$\frac{21}{34}$
1	0.941	0.853	0.794	0.764	0.735	0.676	0.647	0.618
0	$\frac{1}{2}$	1	$1\frac{1}{2}$	2	$2\frac{1}{2}$	3	$3\frac{1}{2}$	4

The apparent quantization of bond order corresponds to the numerators in Farey sequences that converge to the golden ratio. As the limiting Fibonacci fraction $n/(n+1) \to \tau$, approaches the golden ratio, the values of quantized bond order, predicted by the Farey sequence $\mathscr{F}_{n+1}$ approach the simulation of Fig. 4.

The simulation described here gives new meaning to the bond-order concept. It now emerges as the quantization of interatomic distance within molecular diatomic domains.

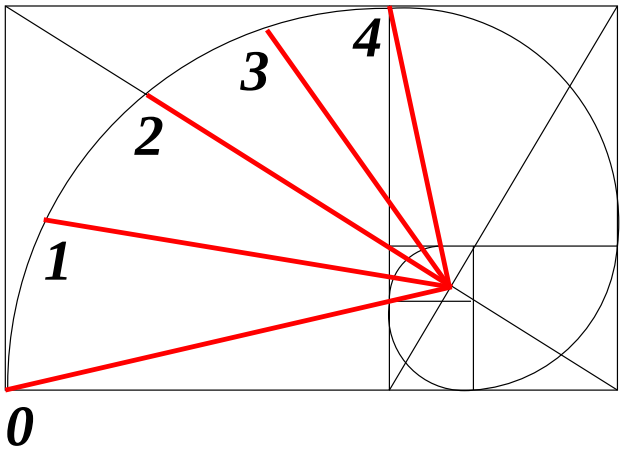

Fig. 4 Simulation of integer bond orders on a golden logarithmic spiral

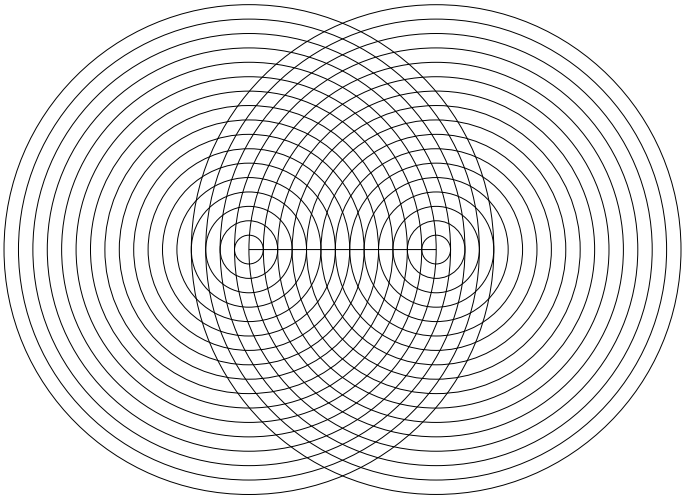

Fig. 5 Wave structure that defines second-order homonuclear interaction.

The quantization results from constructive interference between the valence-electron waves of interacting atoms of opposite spin. The interference pattern for second-order homonuclear interaction, $d' = 26/34 \equiv 13/17$, is shown in Fig. 5. Only even numbered wave crests are shown. Bond order changes in regular steps as the dimensionless interatomic distace, d' changes in steps of 1/34, which define the wavelength of the spherical waves. For C and H with respective values of $r_0 = 1.78$ and 0.97 Å, wavelengths of $\lambda(\mathrm{C}) = 1.78/34 = 5.24 \times 10^{-12}$ m and

$\lambda(\mathrm{H}) = 2.86 \times 10^{-12}$ m are predicted. This result is in winsome agreement with the Compton wavelength of an electron at 2.43×10^{-12} m.

Gaps in the 21/34 sequence of bond orders suggest the possibility of intermediate bond orders at 31/34, 28/34 and 24/34. This conclusion is supported by the comparison (Table 5) with the bond orders predicted by Table 2. One finds:

Table 5 Comparison of different estimates of bond order.

n	33	32	31	30	29	28	27	26	25	24	23	22	21
$1000n/34$	971	941	912	882	853	823	794	764	735	706	676	647	τ
Mean		941			868		809			721		662	
Table 2		935			869		804	764		724	683	658	τ
B.O		$\frac{1}{2}$			1		$1\frac{1}{2}$	2		$2\frac{1}{2}$	3	$3\frac{1}{2}$	4

The two calculations converge and confirm earlier empirical conclusions:

- Between bond orders 0 and 1 there is a broad, poorly resolved, shallow minimum of weak interactions, collectively assigned to bond order $\frac{1}{2}$;
- Bond orders 2 and 4 are well resolved;
- Bond orders 1, $1\frac{1}{2}$, $2\frac{1}{2}$ are less sharply defined, but within clear limits;
- Bond orders 3 and $3\frac{1}{2}$ are poorly resolved;
- The $\mathscr{F}_{34}$ sequence specifies an absolute measure of bond order, but the Table 2 values are more convenient in practice.

The idea of bond lengths that may vary around special integer bond orders was first proposed on empirical grounds [24].

The findings reported here provide new evidence for the unity of micro- and macro-physics, and refute the perception of separate quantum and classical domains. The known universe exists as a four-dimensional space-time manifold, but is observed in local projection as three-dimensional Euclidean tangent space that evolves in universal time. The observable world, at either micro or macro scale, can be described in either four-dimensional (non-classical) or in classical three-dimensional detail. The descriptive model may change, but the reality stays the same. This realization is at the root of self-similarity between large and small. The symmetry operator, which reflects the topology of space-time, is the golden logarithmic spiral.

Cosmic self-similarity has been documented and discussed many times with reference to atomic nuclei, atomic structure, the periodicity of matter, covalence, molecular conformation [25], biological structures, planetary and solar systems [26], spiral galaxies and galactic clusters [27]. The prominent role of the golden ratio in all cases can only mean that it must be a topological feature of space-time structure.

The simplest and most beautiful illustration of golden-ratio self-similarity must surely be the quantization of bond order, shown in Figs 3 and 4. It is so intimately entangled with golden symmetry and gives such a precise definition of the otherwise elusive bond-order concept that the possibility of this being mere coincidence is zero. Small wonder that the great Johannes Kepler referred to the ″divine proportion″ which ″served as idea to the Creator when He introduced the creation of likeness out of likeness, which also continues indefinitely″.

In the same spirit the construction of Fig.5, which has nothing to do with chemistry, may well be used as a starting point from which to derive a theory of covalent interaction, atomic structure, elemental periodicity and molecular shape. Working backwards through the concepts developed before [6, 5, 25] a complete framework of chemistry may be developed as a theme in pure number theory.

The natural limit to bond order , which occrs at $d' = \tau$, $D' = 2\tau$, as a result of the wave nature of electrons, is inferred to reflect the topological property that limits electron density in space-time to a natural maximum. It is the molecular counterpart of the property that limits the total charge density at the electronic energy levels on an atom. The empirical rule, known as Pauli's exclusion principle, is formulated in terms of either spin pairing or the antisymmetry of four-dimensional wave functions, which amount to the same thing. As currently understood, it appears as an emergent property of matter waves, with its origin in space-time topology.

3 Homonuclear Interaction

For ease of reference we tabulate atomic ionization radius (r_0), bond order (b) and exponents (n) of lowest-order observed homonuclear interactions in Table 6.

Based on the parameters in Table 6 calculated parameters for homonuclear low-order interactions and diatomic molecules are compared with experimental data in Table 7. Calculation involves the characteristic atomic radii, r_0, and the scale factors based on the golden ratio :

$$d_c = d'_b r_0$$
$$D_c = K r_0^2 \tau^n .$$

Having tested these formulae exhaustively against all spectroscopic and crystallographic data in HCP [7] it is found that they work without serious exception. The bond-order relationship between d and D holds generally, but a few cases deserve special mention.

The relationship is most sensitive for the small atoms of period 2. Based on dissociation energies the atoms B to F have the exponent $n = 6$, except for C with $n = 5$. Judging by interatomic distance however, B and C appear to be of first order whereas O, N and F have $b = \frac{1}{2}$. We interpret this trend in terms of increasing spectator electron density in the relatively small valence shells of these atoms. The dissociation energies seem to indicate a gradual descrease in bond order from C to

F, of the form: $1, <1, > \frac{1}{2}, \frac{1}{2}$. Higher-order bonds of these atoms will be shown to have golden exponents $n = 6 - b$.

The exponent $n = 8.5$ indicates $b = \frac{1}{2}$ for Cu, but the observed interatomic distance of 2.22Å in diatomic Cu_2 is typically first order, in line with the variability exposed in Table 5.

Metals of the second and third transition series are well known to be characterized by multiple dimetal interactions of orders 3, $3\frac{1}{2}$, and 4 [28]. The large reported

Table 6 Parameters r_0/Å, b and n

	Li	Be	B	C	N	O	F	Ne		
r_0	2.36	2.20	1.88	1.78	1.69	1.60	1.52	1.44		
b	<0		1	1	$\frac{1}{2}$	$\frac{1}{2}$	$\frac{1}{2}$			
n	9	10	6	5	6	6	6	14		
	Na	Mg	Al	Si	P	S	Cl	Ar	K	Ca
r_0	3.09	2.87	2.74	2.62	2.51	2.47	2.30	2.21	3.50	3.09
b	0		$\frac{1}{2}$	1	2	1	1		<0	
n	11	12	9	7	6	7	7	15	12	13
	Sc	Ti	V	Cr	Mn	Fe	Co	Ni		
r_0	3.02	2.99	2.96	3.02	2.90	2.87	2.85	2.81		
b	1	1	2	1	$\frac{1}{2}$	1	1	2		
n	9	9	8	9	10	9	9	8		
	Cu	Zn	Ga	Ge	As	Se	Br	Kr	Rb	Sr
r_0	2.88	2.76	3.00	2.89	2.80	2.71	2.61	2.52	3.81	3.54
b	1		0	1	1	1	1			
n	8.5	13	10	8	8	8	8	15	13	14
	Y	Zr	Nb	Mo	Tc	Ru	Rh	Pd		
r_0	3.27	3.24	3.30	3.26	3.14	3.20	3.16	~ 2.5		
b	1	3	4	$3\frac{1}{2}/4$	$3/3\frac{1}{2}$	$3/3\frac{1}{2}$	2	2		
n	9.5	8	7	7.5/7	8/7.5	8/7.5	8.5	8.5		
	Ag	Cd	In	Sn	Sb	Te	I	Xe		
r_0	3.11	3.00	3.31	3.19	3.09	2.98	2.88	2.75		
b	1		0	1	2	2	1			
n	9	15	11	9	8	8	9	15		
	Cs	Ba	La	Ce	Pr	Nd	Pm	Sm		
r_0	4.03	3.75	4.62	4.49	4.68	4.66	4.64	4.63		
b			1	1	$\frac{1}{2}$	0	0	0		
n	13		10	10	11	12				
	Eu	Gd	Tb	Dy	Ho	Er	Tm	Yb		
r_0	4.61	4.51	4.58	4.57	4.55	4.54	4.52	4.50		
b			$\frac{1}{2}$		0					
n	14		11	12.5	12	12.5	13	15		
	Lu	Hf	Ta	W	Re	Os	Ir	Pt		
r_0	3.54	3.50	3.47	3.44	3.40	3.37	3.34	3.41		
b	1	2	$3/3\frac{1}{2}$	<4	$3/3\frac{1}{2}$	$3\frac{1}{2}$	3	$2\frac{1}{2}/3$		
n	10	9	8/7.5	7.3	8/7.5	7.5	8	8.5/8		
	Au	Hg	Tl	Pb	Bi	Po	At	Rn		
r_0	3.38	3.24	3.43	3.32	3.22	3.12	3.03	2.93		
b	2	<0	$\frac{1}{2}$	$\frac{1}{2}$	2					
n	9	15	12	11	9	7				

Table 7 Homonuclear bond length/pm and matching D/kJmol^{-1}

	Li	Be	B	C	N	O	F	Ne		
d_c	*	*	163	155	147	149	142			
d_x	267		159	154	147	148	141			
D_c	102	54	273	397	221	198	179	3		
D_x	110	59	290	377	252	214	159	4		
	Na	Mg	Al	Si	P	S	Cl	Ar	K	Ca
d_c	309	*	256	227	218	214	200		*	*
d_x	308	389	247	232	221	205	199		392	
D_c	66	35	138	328	487	292	253	5	53	25
D_x	75	11	133	310	485	286	243	5	57	17
	Sc	Ti	V	Cr	Mn	Fe	Co	Ni		
d_c	262	260	226	262	271	249	247	215		
d_x	279	252	228	243	300	216	218	217		
D_c	167	163	259	167	95	151	148	233		
D_x	163	118	269	152	81	118	127	204		
	Cu	Zn	Ga	Ge	As	Se	Br	Kr	Rb	Sr
d_c	250	*	300	251	243	235	227		*	*
d_x	222			241	244	232	228		432	
D_c	192	22	100	247	232	217	202	6	38	21
D_x	201	22	106	264	181	223	194	5	49	16
	Y	Zr	Nb	Mo	Tc	Ru	Rh	Pd		
d_c	284	221	203	208	211	215	241	191		
d_x	309	250	210	221	235	231	245	239		
D_c	152	311	520	454	332	344	232	145		
D_x	159	298	513	436	330	331	236	136		
	Ag	Cd	In	Sn	Sb	Te	I	Xe		
d_c	270	*	*	277	268	259	288			
d_x	251					259	268			
D_c	163	7	76	186	282	263	152	7		
D_x	159	7	82	187	302	258	153	7		
	Cs	Ba	La	Ce	Pr	Nd	Pm	Sm		
d_c	*		401	408	438	466				
d_x	470									
D_c	43		240	247	152	94				
D_x	44		247	242	130	84				
	Eu	Gd	Tb	Dy	Ho	Er	Tm	Yb		
d_c	*		428	*	455	*	*			
D_c	35		145	70	89	69	54	20		
D_x	33		132	71	86	75	54	21		
$\pm$	17		25	29	30	29	17	17		
	Lu	Hf	Ta	W	Re	Os	Ir	Pt		
d_c	307	267	233	225	228	220	227	240		
d_x	299	246	223	214	238	233	236	248		
D_c	141	224	405	490	387	427	330	307		
D_x	142		390	486	386	415	361	307		
$\pm$	33		96	96	96	77	68	2		
	Au	Hg	Tl	Pb	Bi	Po	At	Rn		*
d_c	258	*	320	288	246					$> r_0$
d_x	247				266					
D_c	209	10	51	77	190					
D_x	226	8	63	87	197	187				

errors in the measured diatomic dissociation energies for some of these metals are interpreted as due to spectroscopic activation, producing equilibrium mixtures of compounds of poorly resolved bond order. It is noted that in all such cases an average over two bond orders reproduces the experimental data rather well.

Diatomic W_2 provides an interesting demonstration of an interaction which is prevented from reaching bond order 4 ($n = 7$) by the exclusion principle that restricts maximum D' to $2\tau = 1.236$. Since $D'_4 = 1.4 > 2\tau$ n is restricted to the minimum of 7.3.

Observed interatomic distances for diatomic transition-element interactions are estimates of the fraction, $d = 0.78\delta$ of nearest-neighbour approaches in the metals [5] and may be considerably in error in the present context, especially for the second transition series. Apart from first-order La_2 and Ce_2, with $D_x = 245 \pm 30$ kJmol^{-1}, homonuclear diatomics have weak interactions with an average $D_x = 70 \pm 40$ kJmol^{-1}, in agreement with our estimates. Multiple bond orders, in general, are characterized by stepwise reduction of the first-order golden exponent, such that $n_{1+i} = n_1 - i$. Some observed second-order homonuclear interactions in the p-block are collated in Table 8.

Table 8 Comparison of interatomic distance (Å) and dissociation energy/kJmol^{-1} for second-order interaction

	C	O	P	S	As	Se	Sb	Te
d_c	1.36	1.22	1.92	1.89	2.14	2.07	2.36	2.28
d_x	1.34	1.21	1.89	1.89	2.10	2.15		2.56
D_c	642	519	484	472	374	351	282	263
D_x	600	498	485	425	382	331	302	258

Improved estimates of $d = 2.18$ and 2.58 for Se_2 and Te_2 respectively, indicate bond orders of $1\frac{1}{2}$ and 1, rather than 2. The only authentic homonuclear third-order interaction in the p-block occurs for diatomic N_2. It has $d_c = 1.15$Å, $d_x = 1.10$; $D_c = 937$kJmol^{-1}, $D_x = 945$. What is commonly considered to be a triple dicarbon interaction is approximated by $n = 3.16$, as restricted by the 2τ limit. This way $d_c = 1.22$Å, $d_x = 1.21$; $D_c = 964$kJmol^{-1}, $D_x = 966$. The non-existence of a third order diphosphorous interaction is explained directly by noting that it would imply $D' >> 2\tau$.

The dicarbon interaction of order $1\frac{1}{2}$, predicted to have the graphitic $d = 1.40$Å and $D = 505$kJmol^{-1} has been measured in biphenyl with $D_x = 479$kJmol^{-1}.

4 Heteronuclear Interaction

Bond-order analysis of heteronuclear covalent interactions is considerably more complicated, but feasible in principle. An obvious assumption, $R_0 = \sqrt{r_0(1) \cdot r_0(2)}$, predicts correct values for $d = d'_b R_0$ and suggests $D = pKR_0^2\tau^n$. The parameter

$p = \chi(1)/\chi(2)$ is taken as the ratio of electronegativities $\chi(i) \propto r_0^2(i)$ [19] to compensate for polarization effects. Hence

$$D_c = K r_0^3(1)\tau^n / r_0(2)\,,$$

with $r_0(1) > r_0(2)$.

The formulae work surprisingly well when tested against a myriad of examples. A self-consistent set of effective exponents n and bond orders for the p-block is shown in Table 9. Readers are urged to verify the numbers against the large volume of data on heteronuclear diatomic molecules [7], some of which are collated in Table 10. The reported $D_x = 96$ kJmol^{-1} for AsSe appears suspect and has been ignored.

The most interesting molecule in the group is CO, reported to have the strongest covalent bond at 1076 kJmol^{-1}. Classically it is formulated as :C$\overleftarrow{\equiv}$O: , with a so-called dative triple bond. Our formulation is in agreement with such a special structure as a regular third-order interaction would exceed the limit of $D' = 2\tau$ imposed by the exclusion principle. To put the situation into perspective it is noted that on ionization into CO^+ the interatomic distance decreases from 1.128Å to 1.115Å, which seems to imply an increase in bond strength. However, the observed dissociation energy also decreases in the process from 1076 to 806 kJmol^{-1}. Referred to Fig. 1 this CO interaction lies outside the covalent crescent, CBA, which also indicates an additional factor, such as an ionic contribution to the total interaction, at work.

What seems to be happening is that, when prevented from establishing third-order interaction, a rearrangement of the combined valence density occurs in such a way that a more efficient lower-order interference pattern is promoted. Such a rearrangement exists in a modification of the atomic valence spheres. An outward flow of electron density causes a decrease in characteristic radius, and *vice versa*. A decrease of r_0(O)$\rightarrow$ 1.36Å, balanced by an increase of r_0(C)$\rightarrow$ 1.784Å, is found to promote the formation of $2\frac{1}{2}$-order interaction at $R_0 = \sqrt{1.36 \times 1.784} = 1.56$Å, to match the observed $d = 1.56 \times 0.724 = 1.128$Å and dissociation energy $D_x = 1389\tau^{3.5} \times 1.784^3/1.36 = 1076$ kJmol^{-1}, as observed.

Ionization, CO$\rightarrow$CO$^+ + e$, implies decrease of both characteristic radii. At r_0(O)=1.44 and r_0(C)=1.65Å the $2\frac{1}{2}$-order interaction occurs at $R_0 = \sqrt{1.44 \times 1.65} =$ 1.54Å to match the observed $d = 1.54 \times 0.724 = 1.115$Å and dissociation energy $D_c = K\tau^{3.5} \times 1.65^3/1.44 = 804$kJmol^{-1}, as observed. This polarization also explains the observed dipole moment of CO.

The same bonding pattern repeats for all group14–group16 diatomic molecules, that map outside the covalent region of Fig. 1.

4.1 Hydrides

The hydrides constitute the largest group of heteronuclear covalent interactions. Calculated results are in Tables 11 and 12.

Table 9 Bond orders and exponents for diatomic interactions between representative elements

	F	Cl	Br	I	O	S	Se	Te		N	P	As	Sb	Bi
Li	$1\frac{1}{2}$ 6.5	1 6	1 7	$\frac{1}{2}$ 7.5	1 7.5	7			B	$2\frac{1}{2}$ 5.5	7.5			
Na	1 8.5	1 8	$\frac{1}{2}$ 8	$\frac{1}{2}$ 8	$\frac{1}{2}$ 9.5				C	3 4	2 6.5			
K	$\frac{1}{2}$ 9	$\frac{1}{2}$ 8.5	$\frac{1}{2}$ 8.5	$\frac{1}{2}$ 8.5	10				N		$2\frac{1}{2}$ 6.5	2 7.5	7.5	
Rb	$\frac{1}{2}$ 9.5	$\frac{1}{2}$ 9	$\frac{1}{2}$ 9	$\frac{1}{2}$ 9	$\frac{1}{2}$ 10.5				O	3 4	2 6.5	2	8.5	9.5
Cs	$\frac{1}{2}$ 10	$\frac{1}{2}$ 9.5	$\frac{1}{2}$ 9.5	$\frac{1}{2}$ 9.5	$\frac{1}{2}$ 11				F	$1\frac{1}{2}$ 5.5	$1\frac{1}{2}$ 7.5	7.5	1	9.5
Be	1 5.5	6	7.5		$2\frac{1}{2}$ 5	2 7			Al	8	9	8.5		
Mg	1 8	1 7.5	7.5	8	$1\frac{1}{2}$ 8	8.5			Si	2 7.5	7			
Ca	1 8.5	1 8	8.5	$\frac{1}{2}$ 8.5	$1\frac{1}{2}$ 9	$1\frac{1}{2}$ 8.5			P			7	8	9
Sr	1 9	1 8.5	1 8.5	$\frac{1}{2}$ 9	$1\frac{1}{2}$ 9.5	9			S	7	6.5		8	8.5
Ba	1 9.5	$\frac{1}{2}$ 9	$\frac{1}{2}$ 9	$\frac{1}{2}$ 9	$1\frac{1}{2}$ 9	$1\frac{1}{2}$ 9			Cl	$1\frac{1}{2}$ 7	$1\frac{1}{2}$ 7	7		8.5
B	2 5	1 6	1 7.5	$\frac{1}{2}$ 8	3 4	2 6	7	8.5	Ga		8.5	8.5	9	9.5
Al	$1\frac{1}{2}$ 7	1 6.5	1 7	1 7	2 7.5	$1\frac{1}{2}$ 7.5	7	8	As				8	
Ga	$1\frac{1}{2}$ 8	1 7.5	1 7.5	1 7.5	$1\frac{1}{2}$ 8.5			8	Se		7			8.5
In	1 9	1 8.5	1 8.5	1 8.5	9.5	9	9	9	Br	1 8.5	7			9
Tl	1 9.5	1 9	1 9	1 9	10.5				In		9.5	9.5	9.5	9.5
C	2 5	$1\frac{1}{2}$ 6.5	8	9	$2\frac{1}{2}$ 3.5	$2\frac{1}{2}$ 6	2 7		Sn					9
Si	1 7	1 7	7.5	8	$2\frac{1}{2}$ 5.5	2 6	2 6	7	Sb					8.5
Ge	1 8	1 7.5	1 7.5	8	2 7	2 6.5	2 6.5	$1\frac{1}{2}$ 7	Te		8		8	8.5
Sn	1 8.5	1 8.5	8	9	$1\frac{1}{2}$ 8.5	$1\frac{1}{2}$ 7.5	$1\frac{1}{2}$ 8	$1\frac{1}{2}$ 8	Tl		9.5		10	10.5
Pb	$\frac{1}{2}$ 9.5	9	9	9.5	$1\frac{1}{2}$ 9	$1\frac{1}{2}$ 8	$1\frac{1}{2}$ 8.5	$1\frac{1}{2}$ 8.5	Pb					10

4.2 Stretching Force Constants

The calculation of harmonic force constants of covalent bonds has been shown to derive from ionization radii by an equally simple procedure. Following the rule defined as

$$D' = r_0^3 \tau^n \quad , \quad i.e. \quad D_x = K r_0^2 \tau^n$$

Table 10 Calculated and experimental dissociation energies ($kJmol^{-1}$) of heteronulear first-order interactions. Golden exponents *n* are marked by asterisks

	C	N	F	Si	P	Cl	Ge	As	Br	I
C		* 5.5	* 5				248 248			
N	329 329		* 5.5							
O	347 351		208 220			225 206		318 302		
F	465 514	313 < 349				* 6			* 6	* 6.5
Si	298 302		565 567							
S	318 294		293 286			247 256				
Cl	326 336	167 155	270 261	374 349	329 328		310 340	282 294	* 7.5	* 8
As	226 231		427 466							
Se	259 244		304 286							
Br	296 277	118 118	305 280	329 315	267 265	226 219	274 277	249 244		
Sn	205 227					327 319				
Sb	186 197									
I	246 214		266 < 272	270 235	174 185	196 211	194 181	198 181	* 8.5	
Xe			153 130							

it follows directly that for homonuclear interactions

$$k_r = \frac{4.615\tau^+ s}{(\Delta d' \cdot r_0)^2},$$

in which $\tau^+ = \tau^n - \tau^{n+1} = \tau^{n+2}$, n is the bond-order exponent and s the slope of the bond order–$\Delta d'$ function.

In the calculation of heteronuclear interactions it is necessary to substitute $R_0 = \sqrt{r_0(1) \cdot r_0(2)}$. A serious complication exists therein that, as for homonuclear interactions, the critical stretch to effect a change of bond order depends on atomic volume and, in addition, also on relative atomic size. The strategy to address this problem was to use known parameters, together with experimental force constants, to calculate effective values of $\Delta d'$ from the expression

$$(\Delta d')^2 = \frac{4.615\tau^+ s}{r_0(1)\cdot r_0(2)\cdot k_r}\,.$$

The calculated values of $\Delta d'$ for heteronuclear diatomics from period 2:

	N	O	F
C	0.72(3)	0.78(3)	0.86(2)
N		0.77(3)	
Be		0.70($2\frac{1}{2}$)	

with bond order in parentheses, appear to be well ordered. In the same way the results for group 2–group 3 diatomics are considered sufficiently alike to assume $\Delta d' = 0.047$ as a predictor in calculating unknown k_r for this family, including compounds of N:

Table 11 Bond order and interatomic distance in H–X interactions

	Li	Be	B	C	N	O	F
R_0/Å	1.59	1.47	1.35	1.31	1.28	1.25	1.21
b	0	0	$\frac{1}{2}$	1	$1\frac{1}{2}$	$1\frac{1}{2}$	2
d/Å		1.47	1.26	1.14	1.01	0.98	0.92
Obs	1.60	1.34	1.23	1.12	1.04	0.97	0.92
	Na	Mg	Al	Si	P	S	Cl
R_0	1.73	1.68	1.63	1.59	1.56	1.55	1.49
n	<0	0	0	$\frac{1}{2}$	$\frac{1}{2}$	1	1
d		1.68	1.63	1.48	1.45	1.34	1.30
Obs	1.89	1.73	1.65	1.52	1.42	1.34	1.27
	K	Ca	Ga	Ge	As	Se	Br
R_0	1.84	1.74	1.71	1.67	1.65	1.62	1.59
n	<0	<0	0	$\frac{1}{2}$	$\frac{1}{2}$	$\frac{1}{2}$	1
d			1.71	1.56	1.49	1.51	1.38
Obs	2.44	2.00	1.67	1.59	1.51	1.47	1.41
	Rb	Sr	In	Sn	Sb	Te	I
R_0	1.92	1.86	1.79	1.76	1.73	1.70	1.67
n	<0	<0	0	0	0	0	$\frac{1}{2}$
d			1.79	1.76	1.73	1.70	1.56
Obs	2.37	2.15	1.84	1.78	1.70		1.61
	Cs	Ba	Tl	Pb	Bi	Au	Hg
R_0	1.98	1.92	1.82	1.79	1.77	1.81	1.77
n	<0	<0	0	0	0	1	0
d			1.82	1.79	1.77	1.57	1.77
Obs	2.49	2.23	1.86	1.80	1.75	1.52	1.74
	Cr	Mn	Ni	Cu	Zn	Ag	Cd
R_0	1.71	1.68	1.65	1.67	1.64	1.74	1.71
n	0	0	1	1	0	$\frac{1}{2}$	0
d	1.71	1.68	1.43	1.45	1.64	1.62	1.71
Obs	1.67	1.73	1.47	1.46	1.59	1.62	1.76

Table 12 Calculated and experimental dissociation energies ($kJmol^{-1}$) of H–X interactions

	Li	Be	B	C	N	O	F	
n	9	8	7	6.5	6.5	5.5	4.5	
D_c	248	201	327	353	303	416	577	
D_x	238	200	340	338	< 339	430	570	
	Na	Mg	Al	Si	P	S	Cl	Cu
n	11.5	11.5	9.5	9.5	9	8.5	7.5	10
D_c	167	136	303	265	298	360	472	277
D_x	186	126	288	293	297	354	431	255
	K	Ca	Ga	Ge	As	Se	Br	Ag
n	12	11.5	10.5	10	10	9.5	9	10.5
D_c	190	167	247	280	255	294	336	276
D_x	181	223	276	263	274	313	366	244
	Rb	Sr	In	Sn	Sb	Te	I	Au
n	13	12.5	11	11	10.5	10.5	10	10.5
D_c	150	152	260	232	270	243	277	353
D_x	167	165	243	264	240	260	298	311
$\pm$	21	8		17		7		
	Cs	Ba	Tl	Pb	Bi	Zn	Cd	Hg
n	13	12.5	12	12	(11)	13	13	15
D_c	178	182	179	162		82	73	34
D_x	175	192	195	≤ 157	< 283	86	69	40
$\pm$			4					
	Sc	Ti	V	Cr	Mn	Fe	Co	Ni
n	11	11	11	11	10.5	11	10	10
D_c	197	191	186	197	224	169	268	257
D_x	205	205	209	190	251	148	245	240
$\pm$	17	9	7					8
	Pt	Yb	Nb	Mo		Ru	Rh	Pd
n	9.5	14	11	11.5		11	11	9.5
D_c	363	157	257	206		235	226	230
D_x	327	159	> 222	211		223	241	234
$\pm$		38				15	6	25

	C	N	O
Mg			$0.047(2\frac{1}{2})$
Si			$0.051(2\frac{1}{2})$
P	0.045(2)		0.044(2)
S	$0.046(2\frac{1}{2})$		0.047(2)

A similar regularity which emerges for heteronuclear halides:

	Cl	Br	I
F	0.09	0.08	
Cl		0.07	
C	0.08	0.06	0.05

confirms that the algorithm yields reasonable results.

4.2.1 Hydrides

The hydrides of *p*-block elements represent the best documented set of experimental stretching force constants. The previous strategy yields the surprising result that, as for homonuclear interactions, the effective critical stretch $\Delta d'$ is a function of only bond order. In the first linear region, $s = 1.3$, the value $\Delta d' = 0.115$, with bond orders as identified in Table 11, predicts the following force constants:

BH : $k_r = 3.28$	($k_x = 3.05$ Ncm^{-1}	
CH :	4.39	4.48
NH :	4.62	5.97
OH :	7.92	7.80
FH :	9.64	9.66

With the exception of NH this is considered excellent agreement.

In the second period $\Delta d' = 0.062$ predicts k_r in exact agreement with experiment: SH= 4.22, PH= 3.21 Ncm^{-1}. Calculating back from the observed k_r for the hydrogen halides, F to I, the sequence $\Delta d' = 0.115$, 0.073, 0.054, 0.046 appears reasonable.

These results are in line with the small ionization radius of hydrogen, which shows that its entire charge sphere becomes embedded into a larger sphere on molecular formation. The effective point position of the proton relative to the wave structure of the larger atom decides the bond order.

4.3 Molecular Hydrogen

For H alone the ionization radius is known as an analytical result, $r_0 = 1.835 \times 0.53 = 0.97$Å. Experimental parameters for H_2 are:

$$D_x = 436\,\text{kJmol}^{-1}$$
$$d = 0.74\,\text{Å}$$
$$k_r = 5.75\,\text{Ncm}^{-1}$$

The interatomic distance defines $d' = 0.74/0.97 = 0.763$, which corresponds precisely to bond order 2, with the interesting corollary $d' = 2\tau^2$. Sadly, as inferred from simple number theory, the $D_c = 1389 r_0^2 \tau^2 = 499$ kJmol^{-1} does not match the observed.

The factor $\tau^{2.28} \simeq \frac{1}{3}$ produces the observed D_x. It is noted that another molecular form, the familiar H_2^+, has $D_x = 269 \simeq 1389 r_0^2/5 = 261$ kJ, and with $d' = 1.09$, bond order $b < 0$. The intermediate first-order excited state with $d = 0.84$Å and $D = 1389 r_0^2/4 = 327$ kJmol^{-1} has not been observed.

The observed deviation of the golden exponential from the expected integral value of 2 suggests some exclusion principle that prevents exact second-order in-

teraction. It is shown in Fig. 6 how the superposition of two spherical waves of wavelength $\lambda = a_0/2$ predicts constructive interference at $3\lambda = 0.795$ rather than 0.74Å, required for $b = 2$. The mismatch is responsible for the shift to $\tau^{2.28} \simeq \frac{1}{3}$,

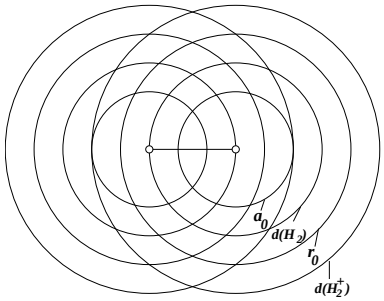

Fig. 6 Graphical simulation of the *H–H* interaction

which in real terms is an almost imperceptable deviation from second-order interaction.

An obvious simulation of the stretching force constant for H_2 would be in terms of the stretch $\Delta d' = 1.09 - 0.763 = 0.327$, $\tau^{4.28} \simeq \tau^2/3 = 0.1275$ and unit initial slope:

$$k_r = \frac{4.615 \times 0.1275}{(0.97 \times 0.327)^2} = 5.85\,,$$

compared to $k_x = 5.75$ Ncm^{-1}.

In order to understand the results reported here it is imperative to abandon the idea of bond order as a function of electron pairs. The alternative definition in terms of wave structures clarifies many a puzzling feature of conventional theory, such as the relative strengths of electron-pair bonds of the same order. By inspection, the variation of experimental covalence parameters D, d and k_r, shown in Table 13, are qualitatively at variance with a constant bond order of unity as required by the electron-pair model.

Table 13 Variation of parameters with bond order

		H	B	C	N	O	F
	D	436	340	338	< 339	430	570
	d	0.74	1.23	1.12	1.04	0.97	0.92
H	k_r	5.75	3.05	4.4 8	5.97	7.80	9.66
	b	2	$\frac{1}{2}$	1	$1\frac{1}{2}$	$1\frac{1}{2}$	2
	n	2.28	7	6.5	6.5	5.5	4.5
	D	570	732	514	< 349	220	159
	d	0.92	1.26	1.40	1.41	1.42	1.41
F	k_r	9.66		7.42			4.70
	b	2	2	1	1	$\frac{1}{2}$	$\frac{1}{2}$
	n	4.5	4.5	5	5.5	6	6

However, in terms of the alternative bond order parameters b and the golden exponents n these quantities are correctly simulated at the quantitative level. The mystery that surrounds many other observations such as the paramagnetism of molecular oxygen or the non-existence of a P_2 triple bond also disappears.

5 Diatomic Dipole Moments

It has been shown that the electronic charge distribution in an atom is readily calculated by the same optimization procedure, based on a golden spiral [6], that correctly predicts all satellite orbits in the solar system [26]. The simulation is sufficiently reliable to enable an improved derivation of the ionization radii of compressed atoms [18], known to generate a self-consistent electronegativity scale [19]. Having demonstrated that the same elements of number theory also dictate the details of atomic periodicity and the nature of covalent interaction, without the use of higher mathematics, it is of interest to also explore the feasibility of calculating molecular dipole moments by the same approach. The results for diatomic molecules are compared to the data tabulated in HCP [7].

5.1 The Algorithm

The formation of a diatomic molecule involves the interaction between two activated valence electrons. In the case of heteropolar interaction the difference in quantum potential energy (electronegativity) of these two electrons results in a skewed charge distribution, which may be expressed as a difference δQ in charge, measured at the nuclear sites.

The dipole moment of a diatomic molecule is defined as the product of equal, but electrically opposite, fractional charges at the interatomic distance d apart, *i.e.*

$$\mu = \delta Q \cdot d\,.$$

The magnitude of δQ depends on the differences in atomic electronegativities, polarizabilities and valence densities. The effect of different electronegativities has been considered in the calculation of dissociation energy and is introduced here for a single electron as

$$p^+ = \sqrt{r_0^3(1)/r_0(2)} \qquad \text{together with} \qquad p^- = \sqrt{r_0^3(2)/r_0(1)}\,,$$

the reverse polarization. This defines the polarization factor $\alpha = p^+/v_1 - p^-/v_2$, where v_i is the number of valence electrons on atom i.

In order to estimate atomic polarizabilities it is noted that the inverse of charge density at the crests of the spherical-wave representation of atoms, in units of a_0^3/e,

should be such a measure. This quantity has been calculated before [6] from a spherical standing-wave model of the atom, shown schematically as a radial projection in Fig. 7.

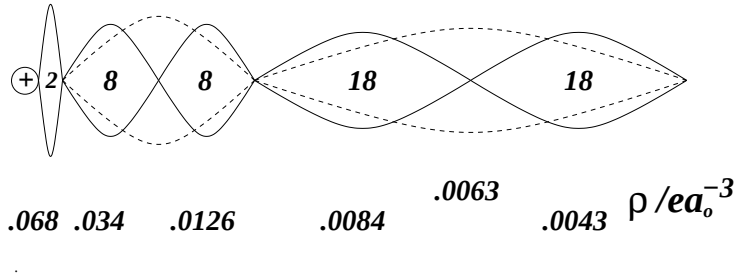

Fig. 7 Electron charge densities in spherical-wave model of the atom

The reciprocals come out as

$$\frac{1}{\rho_n} = 14.7, 29.42, 79.37, 119.04, 158.73, 232.55$$

These numbers are converted into a series of integers

$$\frac{1.02}{\rho_n} \simeq 15, 30, 80, 120, 160, 240 = m$$

which will be used as coefficients to calculate polarizabilities directly from ionization radii; noting that the quantity $k = m/nr_0$ oscillates about $k \simeq 10$ for period number n, as shown in Table 14.

In this table units of a_0^3/e and Å^{-1} are mixed. To ensure consistency we convert $1\text{Å}^3 = (0.52)^{-3}a_0^3 = 7.11a_0^3$. Also, calculated charge densities refer to fully occupied energy levels, whereas the $1/r_0$ simulation specifies one-electron densities. The ratio $f(1:8) \to 1.38$, compensates for this effect, to give the complete conversion factor $k = 7.11 \times 1.38 = 9.81$, that generates the numbers $a_n = m/10$ from $1/\rho_n$. From these numbers polarizabilities are calculated as $s_n = a_n/r_0(n) = f/10$ of Table 14. This result provides a simple conversion of calculated dipole moments into Debye units. Noting that

$$1D \equiv 3.336 \times 10^{-30}\text{Cm}$$
$$1e\text{Å} = 4.8\text{D},$$

the dimensional constant for conversion of dipole moments into Debye units follows directly as $K = 10/3.336 = 3$.

Table 14 Numerical relationship between ionization radii and atomic polarizabilities. Ionization radii have been calculated by the spherical-wave model [6].

$\frac{15}{r_0}$							H 15.5		Ratio $f(1:8)$
$\frac{30}{2r_0}$	Li 6.4	Be 7.0	B 8.0	C 8.4	N 8.9	O 9.4	F 9.9	Ne 10.4	 1.63
$\frac{80}{3r_0}$	Na 8.6	Mg 9.6	Al 9.7	Si 10.2	P 10.6	S 10.8	Cl 11.6	Ar 12.1	 1.40
$\frac{120}{4r_0}$	K 8.6	Ca 9.1	Ga 10.0	Ge 10.4	As 10.7	Se 11.1	Br 11.5	Kr 11.9	 1.38
$\frac{160}{5r_0}$	Rb 8.4	Sr 9.0	In 9.7	Sn 10.0	Sb 10.4	Te 10.7	I 11.1	Xe 11.6	 1.38
$\frac{240}{6r_0}$	Cs 9.9	Ba 10.5	Tl 11.7	Pb 12.0	Bi 12.4	Po 12.8	At 13.2	Rn 13.7	 1.38

5.2 Results

5.2.1 Interactions of $s-p$ type

Valence density depends on the periodic position of an atom, shown for representative elements in Table 14. The simplest situation to model is the polarization that occurs in an alkali halide molecule, also responsible for the largest dipole moments of diatomic molecules. In effect, a singly-charged valence shell interacts with a single vacancy in the valence shell of the halogen atom. The polarization of the alkali shell should decrease with atomic size, which is measured by the period number of the valence shell. The implied decrease in valence density from Li to Na, of $8.6/6.4 \sim 3/2$, suggests $\nu = 1/n$ as approximate scale factor, which could be complicated by the appearance of d and f sub-levels. It is a complementary vacancy density that should be taken into account.

The feasibility of these assumptions are validated by calculating a dipole moment for LiF with $n = 2$, $s = 3/\big(2r_0(F)\big) \simeq 1$, $K = 3$, $\alpha = 2.77$, $d = 1.56$Å:

$$\mu_c = 3 \times \tfrac{1}{2} \times 2.77 \times 1.56 = 6.48\,,$$

compared to the experimentally measured $\mu_x = 6.33$D. The assumptions also predict the dipole moments of other alkali fluorides with remarkable accuracy. Using $\delta q = 3/n$ for Na to Cs calculates:

$$\mu(\mathrm{NaF}) = (\nu = 1)(n = 3) \times (\alpha = 4.26) \times (d = 1.93) = 8.2 \quad (\mu_x = 8.2\mathrm{D})$$
$$\mu(\mathrm{KF}) = 0.75 \times 5.17 \times 2.17 = 8.4 \quad (\mu_x = 8.6\mathrm{D})$$
$$\mu(\mathrm{RbF}) = 0.6 \times 5.89 \times 2.27 = 8.0 \quad (\mu_x = 8.5\mathrm{D})$$
$$\mu(\mathrm{CsF}) = 0.5 \times 6.43 \times 2.35 = 7.6 \quad (\mu_x = 7.9\mathrm{D})$$

For the higher halides of Li and Na it is adequate to assume $\delta q = 3.5/n$, in line with Table 14.

A better simulation for the higher fluorides $(n > 3)$ is obtained by the physically more sensible assumption of $\delta q \propto V_0(\mathrm{M})/V_0(\mathrm{F})$, *e.g.* $s(\mathrm{KF}) \propto [r_0(\mathrm{K})/r_0(\mathrm{F})]^3 = 12.2$. Noting the factor n^2 that defines wave nodes, we calculate $\delta q = s/n^2$, *i.e.*:

$$\delta q(\mathrm{KF}) = 0.76, \quad \mu_c = 8.53\mathrm{D}$$
$$\delta q(\mathrm{RbF}) = 0.63, \quad \mu_c = 8.42\mathrm{D}$$
$$\delta q(\mathrm{CsF}) = 0.52, \quad \mu_c = 7.86\mathrm{D}$$

Deviations from the ideal rule

$$\frac{3}{2r_0(F)} = \frac{8}{3r_0(Cl)} = \frac{12}{4r_0(Br)} = \frac{16}{5r_0(I)} = 1$$

i.e.:

$$\frac{3r_0(Cl)}{r_0(F)} = \frac{16}{3} \quad , \quad \frac{4r_0(Br)}{r_0(F)} = \frac{24}{3} \quad , \quad \frac{5r_0(I)}{r_0(F)} = \frac{32}{3}$$

define the factors that convert volume ratios to the scale, fixed before by

$$\frac{3}{2r_0(F)} \quad \text{as} \quad \frac{nr_0(X)}{r_0(F)}, \quad e.g. \quad \frac{3r_0(Cl)}{r_0(F)} = 4.54, \quad etc.,$$

with factors for Br=6.87 and I=9.47. This way we find:

$$\delta q(\mathrm{LiCl}) = 1.08 \times 4.54/4 = 1.23, \quad \mu_c = 5.1 \quad (\mu_x = 7.1\mathrm{D})$$
$$\delta q(\mathrm{NaCl}) = 1.22, \quad \mu_c = 9.5 \quad (\mu_x = 9.0\mathrm{D})$$
$$\delta q(\mathrm{KCl}) = 1.00, \quad \mu_c = 10.8 \quad (\mu_x = 10.3\mathrm{D})$$
$$\delta q(\mathrm{RbCl}) = 0.83, \quad \mu_c = 10.7 \quad (\mu_x = 10.5\mathrm{D})$$
$$\delta q(\mathrm{CsCl}) = 0.68, \quad \mu_c = 10.1 \quad (\mu_x = 10.4\mathrm{D})$$

As before simple scaling works better for Li and Na. Final results for all alkali halides are collated in Table 15.

The next group of diatomic molecules with non-trivial dipole moments are the alkaline-earth chalconides where polarization involves double the number of valence electrons and vacancies. Taking this into account we calculate dipole mo-

Table 15 Calculated and observed dipole moments (Debye) of the alkali halides.

	F	Cl	Br	I
Li (μ_c)	6.5	7.2	7.0	7.6
μ_x	6.3	7.1	7.3	7.4
Na	8.2	9.1	8.8	8.9
	8.2	9.0	9.1	9.2
K	8.5	10.8	10.9	11.2
	8.6	10.3	10.6	~ 10.8
Rb	8.4	10.7	10.8	11.2
	8.5	10.5		~ 11.5
Cs	7.9	10.1	10.2	10.6
	7.9	10.4		

ments in reasonable agreement with the experimentally known values for MgO = 6.1, SrO = 8.9, BaO = 8.0 and BaS = 10.9D. Defining $\alpha = p^+/2 - p^-/6$, $\delta q = (1/n^2)[V(M)/V(O)] \times 4$ we find:

$$\begin{aligned} &\text{MgO}: \quad \mu = 2.32 \times (\alpha = 1.62) \times (d = 1.75) = 6.2\text{D} \\ &\text{SrO}: \quad \mu = 1.76 \times 2.47 \times 1.92 = 9.0\text{D} \\ &\text{BaO}: \quad \mu = 1.48 \times 2.76 \times 1.94 = 8.0\text{D} \end{aligned}$$

For BaS with $3r_0(S)/r_0(O) = 4.63$, $s = (1/36)[V(\text{Ba})/V(\text{S})] \times 4$:

$$\text{BaS}: \quad \mu = 1.87 \times 2.02 \times 2.51 = 9.5\text{D}$$

The main objective is not to produce exact dipoles moments, using fine-tuned parameters, but rather to demonstrate that a convincing match with experimental measurement can be achieved by the multiplication of three factors that derive from ionization radii and valence densities alone.

5.2.2 The *p*-block diatomics

In the case of group 3 halides only *p* electrons are involved in the interaction. The halogen vacancy is 1/5 of the *p*-density. Hence we calculate the polarizability factor as $\alpha = p^+ - p^-/5$. Whereas the *s*-density of groups 1 and 2 interacts directly with vacancies in the valence shell, the *p*-density of groups 3 and 7 atoms are not separated by a closed-shell arrangement, but by intervening *d*-levels. The number of charges that separate B from Al= 8, Al−Ga= 18, Ga−In= 18 and In−Tl= 32. Between groups 3 and 7 there are always ±4 charges. Instead of scaling the volume ratios by $1/n^2$, the effective scale factors are $m = 8$, 18+4, $32 - 4$, as in Table 16. In the same calculation for some chlorides with known dipole moments a better fit is obtained with $m \simeq 31$, *i.e.*

Table 16 Calculation of dipole mements of group 3 fluorides

	$s=\frac{1}{m}V(\mathrm{M})/V(\mathrm{F})$	$=\delta q$	α	d/Å	μ_c	μ_x(D)
BF	1.89/8	0.24	1.72	1.26	0.5	0.5
AlF	5.89/22	0.27	3.45	1.65	1.54	1.53
GaF	7.69/22	0.35	3.99	1.77	2.47	2.45
InF	10.33/28	0.37	4.67	1.99	3.44	3.40
TlF	11.49/28	0.41	4.95	2.08	4.22	4.23

$$\mu(\mathrm{InCl}) = 2.98 \times 4.54/31 \times (\alpha = 3.59) \times (d = 2.4) = 3.76\,, \quad (\mu_x = 3.79\mathrm{D})$$
$$\mu(\mathrm{TlCl}) = 0.49 \times 3.81 \times 2.48 = 4.59 \quad (4.54)$$
$$\mu(\mathrm{TlI}) = 1.69 \times 9.47/31 \times 3.21 \times 2.81 = 4.66 \quad (4.61)$$

However, the sample is too small to reveal a logical pattern.

Simulation of the dipole moment of CO needs special care. In order to simulate the $2\frac{1}{2}$-order interaction it is necessary to modify the characteristic radii to r_0(C)=1.784Å, r_0(O)=1.36Å, with the number of valence electrons $v_C \simeq v_O \simeq 3$, to give a polarization factor of $\alpha \leq 0.86$, $\delta q = (1.784/1.36)^3/16 = 0.14$, $d = 1.13$Å, $\mu_c \leq 0.14$D. ($\mu_x = -0.11$D). The charge flow from O→C, implied by the modified radii, inverts the sign of the dipole moment, as observed.

In comparison, *ab initio* SCF calculation of μ(CO) with the correct sign, at -0.077D, requires a double-zeta-plus-polarization basis set with 138 doubly excited configurations plus 62 single excitations [29]. The chemical principles involved here are hard to visualize.

Several chalconide diatomics of the carbon group are also subject to similar modification of their atomic valence spheres. Since these effects have not been calculated, an approximation, which assumes a polarization factor of $\alpha = 2(p^+ - p^-)$, calculated with unmodified atomic radii, with the special scale factors shown in Table 17, was found to give results in good agreement with experiment.

Table 17 Dipole moments of group 4 oxides.

	s	δq	α	d/Å	μ_c	μ_x/D
CO	1.38/9	0.153	0.72	1.13	0.12	0.11
SiO	4.39/9	0.488	4.20	1.51	3.09	3.10
GeO	5.89/16	0.368	5.38	1.62	3.21	3.28
SnO	7.93/23	0.345	6.74	1.83	4.25	4.32
PbO	8.93/28	0.319	7.34	1.92	4.50	4.64

In modelling the higher chalconides a factor $nr_0(\mathrm{X})/r_0(\mathrm{O})$ scales the fractional charges $\delta q = s \cdot f(\mathrm{X})$, where f(S)= 4.63, f(Se)6.78 and f(Te)= 9.32, as in Table

18. For selenides and tellurides the empirical fit to known dipole moments are:

Table 18 Dipole moments of group 4 sulphides

	s	δq	α	d/Å	μ_c	μ_x/D
CS	0.37/4	0.43	2.80	1.54	1.85	1.96
SiS	1.19/4	1.38	0.60	1.93	1.60	1.73
GeS	1.60/13	0.57	1.70	2.01	1.95	2.00
SnS	2.15/20	0.50	2.92	2.21	3.23	3.18
PbS	2.43/25	0.45	3.44	2.29	3.55	3.59

$$\text{CSe}: \quad \mu_c = (0.28 \times 6.78/6) \times (\alpha = 3.80) \times (d = 1.68) = 2.02 \quad (\mu_x = 1.99\text{D}$$
$$\text{GeSe}: \quad \mu_c = (1.6 \times 6.78/10) \times 0.72 \times 2.13 = 1.66 \quad (\mu_x = 1.65)$$
$$\text{GeTe}: \quad \mu_c = (0.97 \times 9.31/12) \times 0.36 \times 2.34 = 1.06 \quad (\mu_x = 1.06)$$

The m index that correlates separated fractional charges with volume ratios is an integer that changes in a regular, but still unspecified way, as in

$$\delta q = \frac{1}{m}[V(M)/V(X)]\,,$$

with the relative periodic positions of M and X. The pattern is summarized in the following array:

	F	F	O	Cl	Cl	S	Br	Br	Se
Li B C	4	4	9	4		4	4		6
Na Al Si	9	22	9	9		9	9		
K Ga Ge	16	22	16	16		13	16		10(12Te)
Rb In Sn	25	28	23	25	31	20	25		
Cs Tl Pb	36	28	28	36	31	25	36		

For alkali halides and alkaline-earth chalconides $m = n^2$, where n is the period number of M. Where both atoms are in the p-block m also depends on the periodic position of X.

The dipole moments of the six interhalogen diatomics are modelled well by calculating $\mu_c = \alpha \cdot \delta q \cdot d$, $\alpha = p_+ - p^-$, $\delta q = (3m/20)(V_1/V_2) \equiv 0.15 \times V_1/V_2 \times m$. Hence

$$\mu(\mathrm{FCl}) = 1.59 \times (0.15 \times 0.289 \times 8) \times 1.63 = 0.90 \quad (\mu_x = 0.89\mathrm{D})$$
$$\mu(\mathrm{FBr}) = 2.26 \times (0.15 \times 0.198 \times 12) \times 1.76 = 1.42 \quad (1.42)$$
$$\mu(\mathrm{FI}) = 2.86 \times (0.15 \times 0.147 \times 16) \times 1.91 = 1.93 \quad (1.95)$$
$$\mu(\mathrm{ClBr}) = 0.62 \times (0.15 \times 0.684 \times 4) \times 2.14 = 0.54 \quad (0.52)$$
$$\mu(\mathrm{ClI}) = 1.16 \times (0.15 \times 0.509 \times 6) \times 2.32 = 1.23 \quad (1.24)$$
$$\mu(\mathrm{BrI}) = 0.55 \times (0.15 \times 0.744 \times 5) \times 2.47 = 0.76 \quad (0.73)$$

Diatomic oxygen halides are correctly modelled by assuming $\alpha = p^+ - p^-$, $\delta q = (V_1/V_2) \times 0.18m$, $m(\mathrm{Cl}) = 10$, $m(\mathrm{Br}) = 12$, $m(\mathrm{I}) = 16$, *i.e.*

$$\mu(\mathrm{ClO}) = 1.43 \times 0.607 \times 1.57 = 1.36 \quad (\mu_x = 1.30\mathrm{D})$$
$$\mu(\mathrm{BrO}) = 2.08 \times 0.497 \times 1.72 = 1.78 \quad (1.76)$$
$$\mu\mathrm{IO} = 2.67 \times 0.492 \times 1.87 = 2.46 \quad (2.45)$$

The scale factors that convert halogen interactions to the F-scale suggest an index $m < 2$ for OF. A measured value very close to zero is reported. From this we infer $m \simeq 0.1$. The same m should model the dipole moment of SF. We find

$$\mu(\mathrm{SF}) = 1.73 \times (12 \times 0.23 \times 0.1) \times 1.60 = 0.76 \quad (\mu_x = 0.79\mathrm{D})$$

Other interactions in the *p*-block are empirically modelled by a closely related scheme. We find:

$$\mu = \alpha \times \delta q \times d$$
$$\mu(\mathrm{NO}) = 0.18 \times (4 \times 0.849 \times 0.18) \times 1.15 = 0.13 \quad (\mu_x = 0.16\mathrm{D})$$
$$\mu(\mathrm{NS}) = 1.59 \times (12 \times 0.320 \times 0.20) \times 1.49 = 1.82 \quad (1.81)$$
$$\mu(\mathrm{OS}) = 1.78 \times (12 \times 0.272 \times 0.18) \times 1.48 = 1.55 \quad (1.55)$$
$$\mu(\mathrm{OP}) = 1.86 \times (12 \times 0.259 \times 0.22) \times 1.48 = 1.88 \quad (1.88)$$
$$\mu(\mathrm{NP}) = 1.67 \times (19 \times 0.305 \times 0.19) \times 1.49 = 2.74 \quad (2.75)$$

5.2.3 Diatomic Hydrides

To find a formula for the dipole moments of diatomic hydrides we look at the hydrides of the first short period and calculate

$$\alpha = \frac{r_0^3(\mathrm{X})}{r_0(\mathrm{H})} - \frac{r_0^3(\mathrm{H})}{r_0(\mathrm{X})} \quad \text{and} \quad s = V(\mathrm{H})/V(\mathrm{X})$$

as shown in Table 19. The values of m are clearly derived from $v \times 3$, which is exact

Table 19 Calculation of hydride dipole moments

	C	N	O	F
v	2	3	4	5
α	2.41 – 0.72 1.69	2.23 – 0.73 1.50	2.05 – 0.76 1.29	1.90 – 0.77 1.12
$u=(V_H/V_X)$	0.16	0.19	0.22	0.26
$s=u/\sqrt{v}$	0.11	0.11	0.11	0.116
$\delta q=ms$	0.77	0.88	1.32	1.74
m	7	8	12	15
d/Å	1.12	1.04	0.97	0.92
$\mu=\alpha\cdot\delta q\cdot d$	1.46	1.37	1.65	1.78
μ_x/D	1.46	1.39	1.66	1.83

for HF $[3/2r_0(\mathrm{F})\simeq 1]$ and decreases slightly to the left, noting that $r_0(\mathrm{C})/r_0(\mathrm{F})\simeq 7/3v$.

By the same method, scaling by the factors 4.54 and 4.63, established before, and noting the difference of 2 in the number of vacancies, we calculate:

$$\mu(\mathrm{HCl})=(\alpha=2.91)\times\left(\frac{1}{\sqrt{5}}\times 0.341\times 2\right)\times(d=1.27)=1.11\quad(\mu_x=1.11\mathrm{D})$$

$$\mu(\mathrm{HS})=3.33\times\left(\frac{1}{2}\times 0.278\times 4\right)\times 0.97=1.80\quad(\mu_x=1.83\mathrm{D})$$

In the same way:

$$\mu(\mathrm{HBr})=3.69\times(1/\sqrt{5}\times 0.51\times 6.87)\times 1.41=0.82\quad(\mu_x=0.83\,\mathrm{D})$$

$$\mu(\mathrm{HI})=4.40\times(1/\sqrt{5}\times 0.038\times 9.47\times 2/5)\times 1.61=0.46\quad(\mu_x=0.45\,\mathrm{D})$$

The effective scale factors for hydrogen halides are:

	HF	HCl	HBr	HI
	15	9.08	6.87	3.80
3×	5	3.03	2.29	1.27

On comparison with similar factors for period 2 hydrides, periodic scaling with respect to F is seen to be such that the cross products between these factors as they appear, moving towards C and I respectively, are simple multiples of 3, as in the following array:

$$\begin{array}{ccccc} & \mathrm{C}(2.33) & \mathrm{O}(2.67) & \mathrm{N}(4.0) & \\ \sim & 3 & 6 & 12 & 15\ \mathrm{F} \\ & \mathrm{I}(1.27) & \mathrm{Br}(2.29) & \mathrm{Cl}(3.03) & \end{array}$$

This regularity is the result of a periodic relationship between atomic ionization spheres, also manifested in atomic electronegativities.

5.3 Discussion

The calculation of dipole moments described here differs from all other methods in ignoring nuclear charge. The rationale behind this is that any atom is electrically neutral. During covalent interaction only the extranuclear charge clouds are subject to polarization, which renders heteronuclear diatomics dipolar. As the characteristics of atomic charge clouds are fully characterized by ionization radii and the number of valence electrons, these are the only parameters needed for the calculation of dipole moments of atomic pairs of known periodic positions. Some of the empirical factors introduced here, although poorly understood, are consistent with a regular periodic pattern.

It is only in the case of the alkali halides that a regular pattern in the variation of dipole moment can be identified and interpreted, with some imagination, in terms of the periodic variatian of ionization radii. The paucity of data for other heteropolar combinations prevents generalization of the observed trend. There are some tantalizing indications that implicate the role of intervening transition and inner-transition levels, but to a large extent, each dipole calculation still represents a special case. Realizing that for only about 5% of the possible heteronuclear combinations between representative elements have dipole moments been measured, the data to substantiate any general simulation are clearly insufficient. However, the limited success demonstrated here confirms that the appropriate parameters for the calculation of dipole moments have been identified, although not necessarily quantified.

6 Conclusion

It would be wrong to interpret this work as an effort to gainsay the importance of quantum theory for chemistry. It does the opposite, but questions the methodology that developed from a naïve interpretation of three-dimensional wave mechanics to confirm the electron-pair model of Lewis and the molecular-structure theory of van't Hoff. Even in terms of the probabilistic interpretation of wave mechanics a rigid three-dimensionally structured molecule, with its real molecular orbitals, is undefined. A strategy, based on these concepts and which became known as *Quantum Chemistry*, amounts to a disastrous misreading of quantum theory and has no predictive power beyond its classical basis.

To avoid further confusion it is recommended to use the term *non-classical theory* instead of the unfortunate *quantum mechanics*. Non-classical theory became important after the discovery of the electromagnetic field. The summary of Maxwell's field equations in the form

$$\left(\frac{\partial^2}{\partial x^2} + \frac{\partial^2}{\partial y^2} + \frac{\partial^2}{\partial z^2} - \varepsilon_0 \mu_0 \frac{\partial^2}{\partial t^2} \right) \Phi = 0$$

resembles a three-dimensional wave equation and was interpreted as such, despite Minkowski's demonstration that it defines a four-dimensional field. Noting that $t/\sqrt{\varepsilon_0\mu_0}$ corresponds to a complex space coordinate, $x_0 = it/\sqrt{\varepsilon_0\mu_0}$, the field equation becomes

$$\sum_{j=0}^{3} \frac{\partial^2 \Phi}{\partial x_j^2} = \Box^2 \Phi = 0 \tag{6}$$

Classical Newtonian mechanics is a subset of this four-dimensional non-classical field. Solutions of (6) represent what is colloquially known as either special relativity or quantum theory.

As a quantum theory (6) introduces the angular-momentum-spin function; fundamental to the periodic table of the elements, which has no recognizable basis in three dimensions. Spin is a purely four-dimensional concept without any meaning in the three-dimensional mechanical world of particles. By definition it defines a mathematically allowed local configuration of four-dimensional space-time. Projected into three-dimensional space it appears as a wave packet. Like all wave phenomena it is characterized by discrete variables, observed as quantum numbers. What the philosopher Popper refers to [30] as the ′quantum muddle′ arises from assigning quantum numbers to classical three-dimensional mechanical particles.

The way in which number theory is used here to simulate chemical behaviour is done in the spirit of four-dimensional non-classical theory. This way an interatomic distance does not represent a ′bond length′ in a rigid classical molecule, but an equilibrium situation resulting from the constructive interference between non-classical valence electron waves. The present results do not inaugurate a new chemistry. It is no more than the tip of an iceberg, destined to blossom into something meaningful.

Acknowledgements I gratefully acknowledge the influence of Peter Comba, the only internationally renowned scientist who, not only indulged, but actively encouraged my maverick views for almost two decades.

References

1. Boeyens JCA (1973) J S Afr Chem Inst 26:94.
2. Meyer AM (1988) J Mol Struct (Theochem) 179:83.
3. Boeyens JCA (1980) S Afr J Chem 33:14.
4. Boeyens JCA (2005) New Theories for Chemistry. Elsevier, Amsterdam.
5. Boeyens JCA (2008) Chemistry from First Principles. Springer.com
6. Boeyens JCA (2012) Atomic structure. This volume.
7. Lide DR (ed.) Handbook of Chemistry and Physics, 86th ed., CRC Press.
8. Kekulé A (1861) Lehrbuch der Organiaschen Chemie. Enke, Erlangen.
9. Meyer V (1888) Ber 21:964; 1620.
10. Stewart AW (1922) Some Physico-Chemical Themes. Longmans, London.
11. Sommerfeld A (1924) Atombau und Spektrallinien, 4th ed, Vieweg, Braunschweig.
12. Pauling L (1960) Nature of the chemical bond, 3rd ed., Cornell University Press, Ithaca, p. 113.
13. Boeyens JCA, Schutte CJH (2012) in [14].
14. Putz MV (ed.) (2012) Chemical Information and Computational Challenges in 21st Century. Nova, New York.
15. Boeyens JCA (1982) J Crystall Spectr Res 12:245.
16. Boeyens JCA, Ledwidge DJ (1983) Inorg Chem 22:3587.
17. Boeyens JCA (1973) J S Afr Chem Inst 26:94.
18. Boeyens JCA (1994) J Chem Soc Faraday Trans 90:3377.
19. Boeyens JCA (2008) Z Naturforsch 63b:199.
20. Boeyens JCA, Levendis DC (2008) Number theory and the periodicity of matter. Springer.com.
21. Boeyens JCA, O'Neill FMM (1995) Inorg Chem 34:1988.
    — (1998) Inorg Chem 37:5352.
22. Bacsa J, Boeyens JCA (2000) J Organomet Chem 596:159.
23. Boeyens JCA (1985) Inorg Chem 24:4149.
24. Boeyens JCA, Cotton FA, Han S (1985) Inorg Chem 24:1750.
25. Boeyens JCA (2010) Int J Mol Sci 11:4267.
26. Boeyens JCA (2009) Physics Essays, 22:493.
27. Boeyens JCA (2010) Chemical Cosmology. Springer.com.
28. Cotton FA, Walton RA (1982) Multiple bonds between metal atoms. Wiley, NY.
29. Schaeffer HF III (1972) The electronic structure of atoms and molecules. Addison-Wesley, Reading, Mass.
30. Popper KR (1992) Quantum Theory and the Schism in Physics. Routledge, London.